Status-dependent aging rates in long-lived, social mole-rats are shaped by HPA stress axis

Arne Sahm[1#], Steve Hoffmann[1], Philipp Koch[2], Yoshiyuki Henning[3], Martin Bens[4], Marco Groth[4], Hynek Burda[5,6], Sabine Begall[5], Saskia Ting[7], Moritz Goetz[7], Paul Van Daele[8], Magdalena Staniszewska[9], Jasmin Klose[9], Pedro Fragoso Costa[9], Matthias Platzer[1], Karol Szafranski[2,*], Philip Dammann[3,10,*]

[1] Computational Biology Group, Leibniz Institute on Aging – Fritz Lipmann Institute, Jena, Germany.

[2] Core Facility Life Science Computing, Leibniz Institute on Aging – Fritz Lipmann Institute, Jena, Germany.

[3] Institute of Physiology, University of Duisburg-Essen, University Hospital Essen, Essen, Germany.

[4] Core Facility Sequencing, Leibniz Institute on Aging – Fritz Lipmann Institute, Jena, Germany.

[5] Department of General Zoology, Faculty of Biology, University of Duisburg-Essen, Essen, Germany.

[6] Department of Game Management and Wildlife Biology, Faculty of Forestry and Wood Sciences, Czech University of Life Sciences, Prague, Czech Republic.

[7] University Hospital, Institute of Pathology and Neuropathology, University of Duisburg-Essen, Essen, Germany.

[8] University of South Bohemia, Department of zoology Branišovská 1760, 370 05 České Budějovice, Czech Republic

[9] University Hospital, Department of Nuclear Medicine, University of Duisburg-Essen, Essen, Germany.

[10] University Hospital, Central Animal Laboratory, University of Duisburg-Essen, Essen, Germany.

[#] Corresponding author (email: arne.sahm@leibniz-fli.de)

*shared senior authorship

Abstract

Background

Mole-rat families of the genus *Fukomys* consist of social categories that differ considerably in their life expectancy. In a typical family, only one pair is reproductively active. These animals, called breeders, reach twice the lifespan of non-breeders in captivity.

Results

We used RNA-seq to compare breeders' gene expression profiles across 15 tissues from both sexes in two *Fukomys* species against those of age-matched non-breeders. The gene found to be most affected was *SULT2A1,* whose gene product is well known to deactivate DHEA – a repeatedly proposed "anti-aging hormone". The second most affected gene – again strongly down-regulated in breeders – was *MC2R*, which codes for the adrenocorticotropic hormone (ACTH) receptor, the primary inducer of glucocorticoid production. In line with this, we found the expression of the target genes of the glucocorticoid receptor substantially altered, breeders exhibited lower weight gain, higher bone density, and stronger use of the IGF1/GH axis. In addition to the latter, several anabolic processes such as protein synthesis, myogenesis, and oxidative phosphorylation, were found to be up-regulated in breeders. Also, apoptosis, P53-signaling, proteasome activity, and the immune defense were elevated in breeders. While coagulation was down-regulated, steroid hormone biosynthesis shifted from glucocorticoid to sex steroid production.

Conclusions

Our results highlight the role of the hypothalamic–pituitary–adrenal stress axis in aging, confirm already known promising targets of aging research, and suggest new ones. The observed up-regulation of the IGF1/GH axis in longer-living breeders questions the extent to which findings from short-lived species can be transferred to longer-lived ones.

Keywords

lifespan, *Fukomys*, hypothalamic–pituitary–adrenal axis, ACTHR, ACTH, DHEA, IGF1, growth hormone, differential gene expression

Background

Most of our current understanding of the underlying mechanisms of aging comes from short-lived model species. It is, however, still largely unclear to what extent insights obtained from short-lived organisms can be transferred to long-lived species, such as humans [1, 2]. Comparative approaches, involving species with particularly long healthy lives and seeking the causative mechanisms that distinguish them from shorter-lived relatives try to overcome this limitation [3]. Many studies that involved organisms with particularly long lifespans, e.g., queens in social hymenoptera, birds, bats, African mole-rats, and primates, have produced findings that were not always congruent with established aging theories [1, 3-7].

Species comparisons, however, also have their limitations. Many observed differences between species with differing lifespans are influenced by phylogenetic constraints, eco-physiological differences, or both, rather than being causal for the species-specific differences in aging rate and longevity. Therefore, the results mentioned above would gain much more value if they could be confirmed or falsified in a system in which it is unnecessary to cross the species border, that is, in a species that contains easily distinguishable cohorts with high vs. low longevity.

Bimodal aging occurs naturally in the genus *Fukomys* from the rodent family Bathyergidae (African mole-rats). These animals live in families (often called colonies) of usually consisting of 9 to 16 individuals [8, 9], although single families may occasionally grow considerably larger in some species [10, 11]. Regardless of group size, an established family typically consists of only one breeding pair (the founders of the family, often called king/queen) and their progeny from multiple litters (often called workers). Because of strict avoidance of incest [12], the progeny do not engage in sexual activity in the confines of their natal family, even after reaching sexual maturity. Hence, grown *Fukomys* families are characterized by a subdivision into breeders (the founder pair) and non-breeders (all other family members).

Interestingly, breeders reach the age of 20 years or more in captivity, whereas non-breeders usually die before their tenth birth date (Fig. 1A). This divergence of survival probabilities between breeders and non-breeders is found in all *Fukomys* species studied so far, irrespective of sex. Because no difference in diet or workload has been observed between breeders and non-breeders in captivity, status-specific changes of gene expression after the transition from non-breeder to breeder are considered the most likely explanation of the differing lifespans [13, 14].

In the wild, non-breeders must meet a member of another family by chance to ascend to breeder status; in captivity, the establishment of new breeder pairs is subject to human control. Allowing an animal to breed in captivity can be regarded as a simple experimental intervention that results in an extension of life expectancy of approximately 100%. This extension is far more than most experimental interventions in vertebrates can achieve e.g. by caloric restriction (e.g., [15]) or diets containing resveratrol or rapamycin (e.g., [16, 17]). Furthermore, this relative lifespan extension starts from a non-breeder lifespan that is already more than twice as long as that of the mammalian model organisms most widely used in aging research, such as mice or rats.

Until now, relatively few studies have addressed the potential mechanisms behind this natural status-dependency of aging in *Fukomys* sp. Contrary to the predictions of both the advanced glycation formation theory [18] and the oxidative stress theory of aging [19, 20], markers of protein cross-linking and -oxidation were surprisingly higher in breeders of Ansell´s mole-rats (*F. anselli*) than in age-matched non-breeders [21]. On the other hand, in the Damaraland mole-rat (*F. damarensis*), oxidative damage to proteins and lipids was significantly lower in breeding females than in their non-reproductive counterparts [22], a finding that is compatible with the oxidative stress theory of aging. In good agreement with their overall longevity irrespective of social status, Ansell´s mole-rats produce less thyroxine (T4) and recruit smaller proportions of their total T4 resources into the active unbound form

than do euthyroid mammals. Still, nonetheless the levels of unbound T4 (fT4) do not explain the intraspecific differences in aging rates between *F. anselli* breeders and non-breeders, because the levels of this hormone did not differ between the two cohorts [23]. Closely connected to the topic of this paper is the finding, that non-breeding giant mole-rats (*F. mechowii*) maintain fairly stable gene expression into relative old ages, quite in contrast to the shorter-lived Norway rat [24]. It is, however, still unclear what happens on the gene expression level when an individual attains breeding status.

Interestingly, a recent study by [7] found that the longest-lived rodent, the naked mole-rat *Heterocephalus glaber*, tended globally to show opposite changes in the transition from non-breeders to breeders compared to shorter-lived guinea pigs. *Heterocephalus* and *Fukomys* are similar in their mating and social behavior, but differences appear to exist regarding the effect of breeding on aging rates: until very recently, naked mole-rat non-breeders have been reported to be as long-lived as breeders [25, 26]. In 2018, a lifespan advantage of breeders over non-breeders was reported in females (but not males), yet the divergence of the two groups appeared to be considerably smaller than in *Fukomys* [27] and underlying data is being debated [28]. In summary, status-dependent aging is either absent in *Heterocephalus* or less pronounced than in *Fukomys*.

In this paper, we make use of the bimodal aging pattern in two *Fukomys* species (*F. mechowii* and *F. micklemi*, Fig. 1A) by comparing the gene expression profiles of breeders (n=24) and age-matched non-breeders (n=22) in 16 organs or their substructures (hereinafter referred to as tissues, Fig. S1, Fig. 1B). Our main aim was to identify genes and pathways whose transcript levels are linked to the status-dependent aging-rates and to relate these patterns to insights into aging research obtained in shorter-lived species.

Results

We measured gene expression differences between breeders and non-breeders in two African mole-rat species, *F. mechowii* and *F. micklemi*. Altogether, we performed RNA-seq for 636 tissue samples covering 16 tissue types from both species, sexes, and reproductive states (breeders and non-breeders). Each of the four groups (male/female breeders/non-breeders) of each species consisted of 5 to 7 animals (see Tables S1 –S5 for sample sizes, animal data, and pairing schemes). For each tissue, we conducted a multi-factorial analysis of differentially expressed genes (DEGs): the analysis was based on the variables reproductive state, sex, and species. During this exercise, we focused on the differences between slower-aging breeders and faster-aging non-breeders. This approach increases our statistical power by giving us a four-fold increase of sample size in comparison to species- and sex-specific breeder vs. non-breeder analyses. At the same time, we can additionally reduce the number of false-positive DEGs by restricting the analysis to those breeding status-related genes that show the same direction in both sexes and both species. We deliberately focused on those genes to concentrate our study on universal mechanisms that hold for both sexes and species.

To globally quantify the transcriptomic differences between the reproductive states, we performed three analyses: clustering of the samples based on pairwise correlation, principal variant component analysis, and an overview of the number of DEGs between reproductive states in comparison to DEGs between species and sex. Clustering of the samples based on pairwise correlations showed a full separation of the two species at the highest cluster level (Fig. S1). Below that level, an almost complete separation according to tissues was observed. Within the tissue clusters, the samples did not show a clear-cut separation between sex or breeder/non-breeder status. Accordingly, a principal variance component analysis showed that species, tissue, and the combination of both variables accounted for 98.4 % of the total variance in the data set; individual differences explained 1.4 % of the variance, and

136 only 0.004 % was explained by breeder/non-breeder status (Fig. 2A). Regarding the numbers of DEGs,
137 we found – unsurprisingly considering the aforementioned facts –by far the highest number of DEGs in
138 the species comparison (Fig. 2b). Although in almost every examined tissue the numbers of detected
139 DEGs were also high between sexes, most tissues exhibited very few DEGs due to breeder/non-breeder
140 status. Exceptions were liver, spleen, ovary and, especially, tissues of the endocrine system (adrenal
141 gland, pituitary gland, thyroid), in which the number of DEGs between breeders and non-breeders
142 ranged from more than sixty to several thousand.

143 Next, we evaluated the relevance of reproductive status DEGs for aging and aging-related diseases. For
144 this analysis, we first determined overlaps by using the Digital Aging Atlas (DAA) – a database of genes
145 that show aging-related changes in humans [29]. Across species and sexes, significant overlaps (FDR <
146 0.05, Fisher's exact test) with the DAA were found in three tissues: adrenal gland, ovary and pituitary
147 gland (false discovery rate [FDR] = 0.005, each; Fig. 3A). Among these three endocrine tissues, the DEGs
148 of the ovaries overlapped significantly with those from adrenal ($p=2.8*10^{-27}$) and pituitary glands
149 (p=0.005), but there was no significant overlap between the two glands (Fig. 3A). Thus, together, we
150 found indications for aging-relevant expression changes after the transition from non-breeders to
151 breeders in three tissues of the endocrine system, which presumably affect separate aspects of aging in
152 adrenal and pituitary glands.

153 Moreover, we compared the DEGs with respect to the reproductive status that we identified in *Fukomys*
154 with regard to their direction to transcript-level changes observed in similar experiments using naked
155 mole-rats and guinea pigs [7]. The direction of the status-dependent DEGs regulation in *Fukomys*, as
156 found in this study, was significantly more often the same rather than opposite as in the naked mole-rat
157 (females, 60 %, $p=5.2*10^{-58}$; males, 62 %, $p=10^{-44}$ for females, Fig.3B, Table S6). In the guinea pig, on the
158 contrary, the *Fukomys* reproductive status DEGs were significantly more often regulated in the opposite

direction (females, 57 %, $p=9*10^{-25}$; males, 59 %, $p=4.7*10^{-23}$, Fig. 3B, Table S6). Thus, at the single-gene level, the expression changes linked to reproductive status may affect lifespan differently in long-lived African mole-rats than in shorter-lived guinea pigs.

Beyond the single-gene level, we aimed to identify metabolic pathways and biological functions whose gene expression significantly depends on reproductive status. For this, we used Kyoto Encyclopedia of Genes and Genomes (KEGG) pathways [30], and Molecular Signatures Database (MSigDB) hallmarks [31] as concise knowledge bases. We used a known method that combines all p-values of genes in a given pathway in a threshold-free manner. The advantage of this approach is that it bundles the p-values from test results of individual gene expression differences at the level of pathways (see Methods section for details). Altogether, the gene expression of 55 KEGG pathways and 41 MSigDB hallmarks was significantly affected by reproductive status in at least one tissue (Fig. S3 and S4). Because the individual interpretation of each of these pathways/hallmarks would go beyond the scope of this study, we focus here on those 14 pathways and 13 hallmarks that were significantly different between breeders and non-breeders (FDR < 0.1) in a global analysis across all tissues (Fig. 4). Because many pathways are driven mainly by gene expression in subsets of tissues, we weighted gene-wise the differential expression signals from the various tissues by the respective expression levels in the tissues. For instance, the expression level of the growth hormone (GH) gene *GH1* is known to be almost exclusively expressed in the pituitary glands. In our data set the *GH1* level of the pituitary gland accounted for 99.96 % of the total *GH1* across all tissues. Accordingly, in pathways that contain *GH,* our weighted cross-tissue differential expression signal for this gene is almost exclusively determined by the pituitary gland. On the contrary, a differential expression signal of this gene in another tissue with a very low fraction of the gene's total expression would have almost no impact on the weighted cross-tissue level – even if that signal were very strong (see Methods section for details).

We found strong indications for increase in the activity of certain anabolic functions in breeders: Ribosomal protein expression (hsa03010 Ribosome, hsa03008 Ribosome biogenesis in eukaryotes, Fig. 4A) was elevated in most tissues (and accordingly also in the weighted cross-tissue analysis). In MSigDB hallmarks, the strongest enrichment signal came from MYC targets (HALLMARK_MYC_TARGETS_V1), which can largely be considered a reflection of enhanced ribosomal protein expression and the fact that MYC is a basal transcription factor up-regulating genes involved in protein translation ([32], Fig. 4B). In functional correspondence, we observed an increase in the expression of mitochondrial respiratory chain components (hsa00190 Oxidative Phosphorylation, HALLMARK_OXIDATIVE_PHOSPHORYLATION, Fig. 4A,B). We also found strong indications for increased protein degradation (hsa03050 PROTEASOME, Fig. 4A). This weighted cross-tissue signal was, in contrast to the situation regarding ribosomes, driven mainly by two tissue types: the adrenal gland and the gonads.

To examine whether the simultaneous up-regulation of the ribosome, proteasome, and oxidative phosphorylation is a coordinated regulation, we performed a weighted gene co-expression network analysis (WGCNA) [33] from our gene count data and examined the connectivity between pairs of those KEGG pathways flagged in the weighted cross-tissue analysis. We found that the expression of ribosomal genes (hsa03010) was significantly linked to those of ribosome biogenesis (hsa03008, FDR=$4.59*10^{-3}$), oxidative phosphorylation (hsa00190, FDR=$4.05*10^{-4}$), and proteasome (hsa03050, FDR=$4.59*10^{-3}$), whereas no other examined pathway pair exhibited a significant connectivity (Fig. S5). Interestingly, ribosome, proteasome, and oxidative phosphorylation pathways also shared other characteristics of their differential expression signals: subtle fold-changes, that is, up-regulation of 3 to 9 % on average. Thus, statistically significant signals at the pathway level resulted from relatively small shifts in all genes of these pathways in a seemingly coordinated manner and across multiple tissues (Data S1). In addition, ribosome (hsa03010, in ovary), proteasome (hsa03050, in ovary and adrenal gland), and RNA-transport

(hsa03013, in adrenal gland) are enriched in those *Fukomys* status-dependent DEGs that show, in a similar experimental setting [7], the same direction in both naked mole-rat sexes and the opposite direction in both guinea pig sexes (FDR < 0.05, Fisher's exact test).

The myogenesis hallmark (Fig. 4B) was also found to be up-regulated in breeders. Expectedly, this weighted cross-tissue result was driven mainly by differential expression signals from muscle tissue: muscle from all tissues exhibited the lowest p-value (Fig. 4A), and 15 of 20 up-regulated genes that contributed most to the weighted cross-tissue differential myogenesis signal exhibited their highest expression in muscle. These genes were involved mainly in calcium transport or part of the fast-skeletal muscle-troponin complex (Data S1). A clear exception of this muscle-dominated expression is found in the gene that exhibited the highest relative contribution to the differential myogenesis signal, *insulin-like growth factor 1* (*IGF1*). This gene was found to be expressed most strongly in ovary and liver and was strongly up-regulated in the breeders´ ovaries and adrenal glands (Table 1). *IGF1* codes for a well-known key regulator of anabolic effects such as cell proliferation, myogenesis, and protein synthesis [34, 35] and has a tight functional relation to GH (gene: *GH1*) another key anabolic regulator upstream of *IGF1*; together, these factors form the so-called GH/IGF1 axis [36-41]. Also, *GH1* was strongly up-regulated in breeders in its known principal place of synthesis, the pituitary gland (Table 1).

With xenobiotic metabolism and TNF-α-signaling, two defense hallmarks were also found to be up-regulated in breeders by the weighted cross-tissue analysis (HALLMARK_XENOBIOTIC_METABLISM and HALLMARK_TNFA_SIGNALING_VIA_NFKB, Fig. 4B). The up-regulation of the reactive oxygen species (ROS) hallmark comprising genes coding for proteins that detoxify ROS (HALLMARK_REACTIVE_OXYGEN_SPECIES_PATHWAY, Fig. 4B) falls into a similar category.

Another interesting aspect that was found to be significantly altered in breeders is steroid hormone biosynthesis (hsa00140 Steroid hormone biosynthesis, Fig. 4A). In this case, both up- and down-

regulated genes were in the pathway, and their absolute fold-changes were roughly balanced. Steroid hormones, on the one hand, comprise sex steroids – because these hormones are important players in sexual reproduction, such differences should be expected given the experimental setup. On the other hand, the class of steroid hormones – corticosteroids – has regulatory functions in metabolism, growth, and the cardiovascular system, as well as in the calibration of the immune system and response to stress [42]. The most influential contributor to the differential pathway signal by far on the weighted cross-tissue level was *CYP11A1,* which codes for the (single) enzyme that converts cholesterol to pregnenolone. This is the first and rate-limiting step in steroid hormone synthesis [43]. Because *CYP11A1* was found to be up-regulated in breeders in its main places of synthesis – the gonads and the adrenal gland (Table 1) – it can be assumed that the total output of steroid hormone biosynthesis in breeders is increased. The pattern of up- and down-regulation on the KEGG pathway, however, suggests that sex steroids especially are produced at a higher rate in breeders whereas circulating levels of glucocorticoids – such as cortisol – should be lower than in non-breeders (Fig. S6; see also our discussion on ACTH-R below).

Finally, several pathways flagged by the weighted cross-tissue analysis seem to be derivatives of the above-mentioned differentially expressed pathways instead of representing altered functions on their own. For example, Huntington's (hsa05016), Parkinson's (hsa05012), and Alzheimer's (hsa05010) diseases could, in principle, be interpreted as highly relevant for aging and lifespan. A closer inspection of these pathways reveals, however, that the genes of the mitochondrial respiratory chain – which is the core of the oxidative phosphorylation pathway – are in all three cases the main contributors to the respective differential expression signals (Fig. S7-S9, Data S1). Similarly, we see in the case of fat digestion (hsa04975 Fat digestion and absorption) that two of the three largest contributors to the differential expression signal of that pathway – *ABCG8* and *SCARB1* – are directly involved in the

transport of cholesterol [44, 45]. Therefore, it seems likely that this signal is an expression of the altered steroid hormone biosynthesis rather than indicating altered fat digestion.

Interestingly, three genes, which we had already mentioned as potential regulators during the pathway analysis, also appeared among the ten most clearly altered genes on the weighted cross-tissue level: *GH1, IGF1,* and *CYP11A1* (Table 1). The top two among these ten are *sulfotransferase family 2A member 1* (*SULT2A1*) and *melanocortin 2 receptor* (*MC2R*). SULT2A1 is the main catalyzer of the sulfonation of the steroid hormone dehydroepiandrosterone (DHEA) to its non-active form DHEA-S [46]. DHEA has repeatedly been proposed to be an "anti-aging hormone" because its levels are negatively associated with chronological aging [47-49]. We found that *SULT2A1* is strongly down-regulated in breeders', liver which is also the main location of its enzymatic action. The second candidate, *MC2R*, encodes the adrenocorticotropin (ACTH)-receptor, which is the main inducer of glucocorticoid synthesis and a crucial component of the hypothalamic–pituitary–adrenal (HPA) axis [50]. In humans and many other mammals, prolonged glucocorticoid excess leads to Cushing's syndrome. Affected individuals exhibit muscle weakness, immune suppression, impairment of the GH/IGF1 axis, higher risk of diabetes, cardiovascular disease (hypertension), osteoporosis, decreased fertility, depression, and weight gain [51, 52]. The large overlap of these symptoms with those of aging could explain to some extent that Cushing's syndrome patients exhibit considerably higher mortality rates [53]. We hypothesized that the increased expression of the ACTH receptor in *Fukomys* non-breeders can cause similar expression patterns and consequences (Fig. 5).

Table 1. Top ten genes regarding weighted cross-tissue differential expression signal.

	Weighted cross-tissue			Tissue with highest expression			
	P-value	FDR	Log2-foldchange*	Tissue	% of cross-tissue Expression	FDR	Log2-foldchange*
SULT2A1	0.00E+00	0.000	-3.19	Liver	97.42	5.27E-06	-3.26
MC2R	6.00E-06	0.046	-0.53	Adrenal gland	89.53	8.78E-05	-0.56
INHA	1.60E-05	0.081	1.57	Ovary	67.91	1.54E-05	2.22
INHA – tissue with 2nd highest expression				Testis	27.61	0.56	0.21
CYP11A1	5.90E-05	0.224	0.61	Ovary	45.55	5.49E-05	0.91
CYP11A1 – tissue with 2nd highest expression				Adrenal gland	43.63	1.48E-03	0.47
NLRP14	1.17E-04	0.355	-0.80	Ovary	68.98	2.84E-05	-1.25
NLRP14– tissue with 2nd highest expression				Testis	18.67	0.54	0.19
GH	2.58E-04	0.618	0.45	Pituitary gland	99.96	1.99E-02	0.45
IGF1	3.62E-04	0.618	0.59	Ovary	51.73	1.20E-04	0.76
IGF1– tissue with 2nd highest expression				Liver	36.28	0.39	0.24
ZP4	3.74E-04	0.618	-1.16	Ovary	95.30	1.99E-03	-1.23
TCL1A	5.33E-04	0.618	-1.05	Ovary	90.12	2.14E-03	-1.18
PNLIPRP2	5.69E-04	0.618	1.36	Ovary	76.08	2.23E-03	1.65

* Direction: breeder/non-breeder

Note – tissues are listed if they contribute at least 10% to cross-tissue expression

We tested this hypothesis (Fig. 5) by checking five of its key predictions. Altered *MC2R* expression (Fig. 6A) coincides with higher cortisol levels in hair samples from non-breeding *F. mechowii* than in those from breeders of the same species (Begall et al., in prep.). Furthermore, glucocorticoids such as cortisol exert their effect by binding to the glucocorticoid receptor that, in turn, acts as a transcription factor for many genes [54]. We tested whether the expression of targets of the glucocorticoid-receptor (NR3C1) was significantly altered throughout our data using two gene lists [55]: about three hundred direct target genes of the receptor that were identified by chromatinimmunoprecipitation (i), and about 1300 genes that were found to be differentially expressed depending on the presence or absence of exogenous glucocorticoid (ii). Both gene lists were found to be significantly affected by differential expression at the weighted cross-tissue level (I, $p=0.001$; ii, $p<10^{-9}$) as well as in 5 (i) and 8 (ii) single tissues (Table S7, S8). In line with our hypothesis, we observed that the weight gain in non-breeders

was, on average, twice as strong compared to the weight gain in breeders during the experiment ($p=7.49*10^{-3}$,type II ANOVA, Fig. 6B). In addition, we found a subtle but significant influence of reproductive status on the density of the vertebrae': the vertebrae of breeders were slightly denser than those of age-matched non-breeders (p=0.03 for vertebra T12 only, and p=0.01 across all examined vertebrae L1, L2, and T12; ANOVA, Fig. 6C, Table S11).

Discussion

The vast lifespan differences between *Fukomys* breeders and non-breeders are, according to our RNA-seq data, associated with only subtle global pattern shifts in transcript levels. Concerning the tested explanatory variables (*Fukomys* species, sex, breeding status), we found by far the highest number of DEGs at the level of the species comparison. Although the number of DEGs between the sexes was comparably high in almost each examined tissue, only very few DEGs were found comparing breeders and non-breeders. One exception is the ovary, whose high number of DEGs corresponds well with the disparity in reproductive activity. Other exceptions are liver, spleen, and, especially, the tissues of the endocrine system (adrenal gland, pituitary gland, thyroid), in which the number of DEGs between breeders and non-breeders ranged from more than 100 to more than 2,500.

Changes in the gene expression of the endocrine system are well known to play an important role both in sexual maturation an in aging and the development of aging-associated diseases, e.g., diabetes and cardiovascular diseases [56-58]. This finding fits well with the observation of substantial changes in the endocrine system after the transition from non-breeders to breeders in the related naked mole-rat – one of the key results of a recent study in that species [7]. The dominance of differential expression in endocrine tissue is also plausible insofar as these tissues exert a strong control function for other tissues via hormone release.

306 Steroid hormone biosynthesis exhibits a bipartite pattern in breeders, with up-regulated sex steroid
307 genes and a simultaneous down-regulation of corticosteroid synthesis genes. The former could be
308 expected as a consequence of sexual activity in breeders. For aging, it is, however, interesting that
309 *SULT2A1*, a gene that codes for the specialized sulfotransferase converting the sex steroid DHEA to its
310 non-active form DHEA-S was found to be heavily down-regulated in breeders. DHEA is the most
311 abundant steroid hormone; it serves as a precursor for sex steroid biosynthesis but also has various
312 metabolic functions on its own [59, 60]. DHEA levels decrease continuously during the human aging
313 process to an extent that favors it as an aging biomarker [61, 62]. As a result, an aggressive advertising
314 of DHEA as "anti-aging hormone" in the form of dietary supplements could be observed in recent years
315 [47-49, 60]. Despite conflicting experimental data from various animal studies and clinical trials, a
316 positive effect of DHEA on human health is frequently considered to be likely in the literature. Large-
317 scale and long-term studies, however, are still pending [47, 62, 63]. Interestingly, DHEA is not only
318 described as an aging marker but also as a marker for clinically relevant glucocorticoid excess [64].

319 Regarding corticosteroid synthesis, we hypothesize that the regulation of adrenal gland *MC2R*, coding
320 for the ACTH receptor, is likely to cause a considerable proportion of the overall observed expression
321 patterns and of the lifespan extension in breeders (Fig. 5). As a critical component of the HPA axis, ACTH
322 is a stress hormone that is produced by the pituitary gland and transported by the the blood to the
323 adrenal cortex, where it binds to the ACTH receptor [65]. Subsequently, the ACTH receptor induces the
324 synthesis of glucocorticoids [50], e.g., cortisol, which in turn cause immunosuppressive and various
325 metabolic effects throughout the organism [66]. Although in many mammals (such as humans, dogs,
326 and guinea pigs) glucocorticoid excess disorder, Cushing's syndrome, is caused by overproduction of the
327 hormone ACTH. Our results for *Fukomys* suggest, that the increased levels of the ACTH receptor may
328 lead to symptoms and expression patterns that could resemble some of molecular and phenotypic

aspects of this pathological condition (Fig. 5). Our hypothesis is supported by a number of confirmed downstream effects: the target genes of the glucocorticoid receptor are highly significantly affected by differential gene expression; non-breeder symptoms were similar to those of humans with abnormally elevated glucocorticoid levels: weight gain, decreases in bone density, and impairment of the GH/IGF1 axis (Fig. 5, Fig.6). Interestingly, blocking of the ACTH receptor has been suggested as a treatment for human Cushing's syndrome [67].

We looked for evidence of a regulation upstream of the ACTH receptor. Given the known positive feedback loop between the ACTH receptor and its own ligand, decreased ACTH synthesis in breeders would have been an obvious explanation [68]. We found that the expression of the ACTH polypeptide precursor gene (*POMC*) is unchanged. However, also other post-transcriptional or post-translational mechanisms such as cleaving may influence the ACTH levels in breeders and non-breeders. Of those genes known to be involved in the regulation of *MC2R* [69, 70], we found that only *PRKAR1B* was differentially regulated in the adrenal gland. However, this gene codes for only one of 7 subunits of the involved protein kinase A. Alternative explanations could be that epigenetic modifications, other still unidentified regulators of the transcript level, or both, are responsible for the differential expression.

In the circulatory system, represented by blood and spleen, down-regulation of coagulation factors was observed in breeders. Because coagulation factors are known to be up-regulated during aging in humans mice, rats, and even fish, this can be interpreted as a sign of a more juvenile breeders' transcriptome [71, 72]. Furthermore, the activity of coagulation factors is associated with a higher risk of coronary heart disease [73]. However, we found no obvious histopathological lesions in the hearts or other organs (spleen, kidney, liver, lung) of non-breeders.. Therefore, if down-regulation of coagulation attentuates the aging process in *Fukomys*, it seems to exert its effect only, if at all, at a latter age not investigated here.

Two defense mechanisms were also found to be up-regulated in breeders: xenobiotic metabolism and TNF-α-signaling. Increased TNF-α-signaling often leads to the induction of apoptosis [74]. In line with this, we found that apoptosis and P53-signaling were also up-regulated in breeders. Apoptosis is considered an important anti-cancer mechanism [75, 76]. We hypothesize this to compensate cancerogenic effects of the anabolic alterations described above (especially the up-regulation of the GH/IGF1 axis). In line with this, our more than 30 years' breeding history with several *Fukomys* species in Germany and the Czech Republic suggests that breeders are as "cancer-proof" as non-breeders despite their much longer lifespan (own unpublished data and R. Šumbera, personal communication).

Many anabolic pathways are up-regulated in breeders across tissues: protein biosynthesis, myogenesis, and the GH/IGF1 axis. In line with this finding and with the fact that protein synthesis consumes 30 to 40% of a cell's ATP budget [77], we observed increased expression of mitochondrial respiratory chain components, implying an increase in the capacity for cellular ATP production. On the other hand, protein degradation and clearance by the proteasome are also up-regulated in breeders. The fact that the expression of proteasomal genes is significantly linked to the genes of ribosome biogenesis and oxidative phosphorylation indicates that those processes influence, or even trigger, each other and hence are regulated in a coordinated manner in *Fukomys* mole-rats.

The results of differential expression of anabolic components such as the GH/IGF1 axis are surprising. They fall within a debate in aging research that has been highly controversial over time: based on the well-known fact that the expression and secretion of GH and IGF1 decline with age in humans and other mammals [78], Rudman *et al*. administered synthetic GH to elderly subjects in 1990, thereby reversing a number of aging-associated effects such as expansion of adipose mass [79]. This led to GH being celebrated as an anti-aging drug [36], including dubious commercial offers. Today's aging research, on the contrary, strongly assumes that the enhanced activity of the GH/IGF1 axis accelerates aging and that

its suppression could extend lifespan even in humans [80-82]. In addition to several studies of synthetic GH in humans yielding less convincing results than those of Rudman *et al*., the main reasons for this turn are the results of studies on short-lived model organisms. From worms to mice, the impairment of the GH/IGF1 axis by genetic intervention consistently led to longer lifespans (Table 2), e.g., the up-regulation of Klotho - an IGF1 inhibitor - extended the mouse lifespan by as much as 30 % [83]. As with the impairment of the GH/IGF1 axis, reducing of protein synthesis by decreasing the expression of MYC, a basal transcription factor, extended the mouse lifespan by as much as 20 % [32] whereas the impairment of the respiratory chain by rotenone resulted in prolongation of the killifish lifespan by 15 % [84] (Table 2).

Therefore, it is astonishing that massive up-regulation of these anabolic key components accompanies a lifespan extension of approximately 100 % in long-lived mammals and potentially even contributes to it. Several points could help to resolve this apparent contradiction: First, the up-regulation of anabolic pathways and key genes is at least partially accompanied by the regulation of other mechanisms that could plausibly compensate for deleterious effects. For example, it is, widely assumed that the negative impact of enhanced protein synthesis on lifespan is to a large extent caused by the accumulation of damaged or misfolded proteins, that is also known to contribute to aging-associated neurodegenerative diseases [15, 85, 86]. Up-regulation of the proteasome, as we observed in breeders in a weighted cross-tissue approach and especially in endocrine tissues, is known to counteract these effects by clearing damaged proteins leading to lifespan extension in worm and fly [86]. Enhanced proteasome activity has also been linked with higher longevity of the naked mole-rat compared to the laboratory mouse [87, 88] and in comparative approaches across several mammalian lineages [89]. We hypothesize that the simultaneously high anabolic synthesis and catabolic degradation of proteins will lead to a higher protein turnover rate in breeders and, accompanied with that, a reduced accumulation of damaged and

misfolded proteins. Similarly, it seems plausible that the up-regulation of the mitochondrial respiratory chain (oxidative phosphorylation) in breeders is compensated for by simultaneous up-regulation of the reactive oxygen hallmark: the mitochondrial respiratory chain is the main source of cellular ROS which can damage DNA, proteins and other cellular components [90, 91]; the reactive oxygen hallmark consists by definition of genes that are known to be up-regulated in response to ROS treatments. Unsurprisingly, at least 25 % of these genes code for typical antioxidant enzymes such as thioredoxin, superoxide dismutase, peroxiredoxin, or catalase that can detoxify ROS. Furthermore, the known cancer promoting effects of an enhanced GH/IGF1 axis [36] could, to some extent, be compensated for by up-regulation of apoptosis and p53 signaling, because these are major mechanisms of cancer suppression [92]. More generally, potential lifespan-extending effects of moderate up-regulation of both the GH/IGF1 axis and ROS production can also be viewed in the light of the hormesis hypothesis [93], which postulates that mild stressors can induce overall beneficial adaptive stress responses. In line with these arguments, we found higher resting metabolic rates in breeders compared to non-breeders in *Fukomys anselli* [94], a species closely related to *F. micklemi*.

413 **Table 2.** Behavior of important aging-relevant genes and pathways in this study.

Gene/Pathway	Regulation in indicated direction and species can reduce lifespan	Regulation in indicated direction and species can extend lifespan	Differentially expressed in this study in indicated tissues and direction*	Gene/Pathway is expressed mainly in the following tissues
Growth hormone (*GH1*)	Mouse ↑[1]	Mouse ↓[2], Rat ↓[2]	Pituitary gland ↑	Pituitary gland
Insulin growth factor 1 (*IGF1*)	–	Mouse ↓[2]	Adrenal gland ↑, Ovary ↑	Liver, Ovary
IGF1-receptor (*IGF1R*)	–	Mouse ↓[1], Worm ↓[3], Fly ↓[3]	Adrenal gland ↓, Ovary ↓	Many
Klotho (*KL*)	Mouse ↓[3]	Mouse ↑[3], Worm ↑[3]	Ovary ↓	Endocrine tissue, Kidney
SIRT1	–	Mouse ↑[6], Worm ↑[7], Fly ↑[7]	–	All
MYC	–	Mouse ↓[8]	Thyroid ↑	All
mTOR	–	Mouse ↓[9], Worm↓[9], Fly ↓[9]	Adrenal gland ↓	All
PRKAA2 (AMPK)	–	Worm ↑[9]	–	Many
TP53	Mouse ↑[11], Fly ↑[11]	Worm ↓[11], Mouse ↑[11], Fly ↑[11]	–	All
SOD2	–	Worm ↓[10], Fly ↑[10]	–	All
FOXO3	Fly ↑[12]	–	Ovary ↓, Adrenal gland ↓	All
Protein synthesis	–	Mouse ↓[8], Worm ↓[9], Fly ↓[9]	Many ↑	All
Proteasome	–	Worm ↑[14], Fly ↑[14]	Gonads ↑, Adrenal gland ↑	All
Lysosome	–	Worm ↑[13]	–	All
Respiratory chain	–	Worm↓[15], Fly ↓[16], Killifish ↓[17]	Gonads ↑, Adrenal gland ↑, Blood ↑, Spleen ↑	All
Apoptosis	Mouse ↑[11], Fly ↑[11]	Worm ↓[11], Mouse ↑[11], Fly ↑[11]	Skin ↑, Pituitary gland ↑	All

1 [36], 2 [78], 3 [95], 4 [96], 5 [97], 6 [98], 7 [99], 8 [32], 9 [17], 10 [100], 11 [101], 12 [102], 13 [103], 14 [86], 15 [104], 16 [105],17 [84]
*Direction: breeder/non-breeder
** Direction: old/young
– Either not affecting lifespan or not known to the best of our knowledge (column 1 and 2); no change (column 3)

A second point that could help to resolve this apparent contradiction concerns the time of intervention. The transition from non-breeder to breeder takes place in adulthood, when by far the largest portion of the growth process has already been completed. In contrast, genetic interventions aimed at prolonging the lifespan by inhibiting the GH/IGFH1 axis (Table 2) usually affect the organisms throughout their entire lifespan, including infancy and youth. Therefore, it is still under debate whether the up-regulation of translation and anabolic processes by the GH/IGF1 axis independently enhances growth and aging or enhances aging only secondarily as a consequence of accelerated growth [106]. Our results are an argument for the latter.

A third point is the question of the transferability of knowledge obtained in one species to other species. Most insights into current aging research originate from very short-lived model organisms (Table 2). It is clear, on the other hand, that the observed effects of lifespan-prolonging interventions listed in Table 2 are by far the smallest in the model organisms with the relatively longest lifespans: mice and rats. Compared to most other mammals, however, even mice and rats are short-lived. Given their body weight and an often-used correlation between body weight and lifespan across mammals, their observed maximum lifespan of about four years corresponds to only 51 % (for mice) and 32 % (for rats) of the expected maximum lifespan. In contrast, humans can live as much as 463% as long as they would be expected based on their body weight. This disparity makes them, given this particular model, the most extreme known non-flying mammal species regarding maximum longevity residual [107]. According to current data, *Fukomys* mole-rats reach values of ca. 200 % and thus can be regarded to be closer to humans than to mice or rats in this respect. It is currently unclear to what degree aging

mechanisms and lifespan-affecting interventions that were discovered in short-lived model species apply to organisms that are far more long-lived, as in our experiment (e.g. [1, 2]). It seems reasonable to hypothesize that specific interventions that prolong the lifespan of long-lived organisms may have no major effect in short-lived species, and vice versa. For example, it could be that changes suitable to prolong the life of species with a low cancer-risk (e.g., African mole-rats, blind mole rats) [26, 108, 109] would have no or only a marginal effect in laboratory mice, whose primary cause of natural death is cancer [110]. Therefore, it may also be possible that those gene expression patterns caused by our lifespan-extending intervention in *Fukomys* mole-rats but contradicting the current knowledge obtained from short-lived organisms may highlight differences in aging mechanisms between short-lived and long-lived species.

As a fourth perspective, one could interpret the down-regulation of the GH/IGF1 axis in non-breeders as a byproduct of the apparent up-regulation of the HPA axis in non-breeders, that may well be adaptive in itself. In the wild, non-breeding *Fukomys* mole-rats can maximize their inclusive fitness by either supporting their kin in their natal family or by founding a new family elsewhere. It has therefore been suggested that the shorter lives of non-breeders could be adaptive on the ultimate level if longevity were traded against some other fitness traits, such as competitiveness, to defend colonies against intruders or to enhance their chances for successful dispersal [13]. A constitutively more activated HPA stress axis is expected to offer advantages for both family defense and dispersal but it carries the risk of status-specific aging symptoms, such as muscle weakness, lower GH/IGF1 axis activity, lower bone density etc. in the long run [52]. This effect may become even more pronounced under laboratory conditions where grown non-breeders cannot decide to disperse even if they would like to.

However, even the down-regulation of the GH/IGF-axis may be adaptive in itself for non-breeders if it has the potential to protect them from further damage. Note that for today's conventional view that

stronger activation of the GH/IGF1 axis accelerates aging (Table 2), it is generally challenging that decreasing activity is well documented to correlate with chronological age in a wide range of mammals, including mice, rats, dogs, and humans [78]. Also, decreasing activity correlates, under pathologic conditions such as Cushing's syndrome, with many symptoms akin to aging (Fig. 5). It has been suggested that one solution to this apparent contradiction may be that that the GH/IGF1 axis is adaptively down-regulated in aging organisms as a reaction to already accumulated aging-related symptoms so that additional damage can be avoided [111, 112].

Finally, recent findings of positively selected genes in African mole-rats (family Bathyergidae, containing also *Fukomys* and *Heterocephalus*) could partly explain some of the surprising results. It is striking that translation, and oxidative phosphorylation were among the strongest differentially expressed molecular processes concering the breeding status. Earlier, these processes were also reported to be the most affected by positive selection in the phylogeny of African mole-rats [113]. Furthermore, *IGF1* was one of thirteen genes that were found to be under positive selection in the last common ancestor of the mole-rats. This may indicate that the corresponding mechanisms were evolutionarily adapted to be less detrimental and make their up-regulation more compatible with a long lifespan. Since the mere fact of positive selection does not permit to draw conclusions about the direction of the mechanistic effect, this hypothesis, however, needs to remain speculative.

Conclusions

We performed a comprehensive transcriptome analysis that, for the first time within mammalian species, compared naturally occurring cohorts of species with massively diverging aging rates. The comparison of faster-aging *Fukomys* non-breeders with similar animals that were experimentally elevated to the slower-aging breeder status revealed by far the most robust transcriptome differences

485 within endocrine tissue: adrenal gland, ovary, thyroid, and pituitary gland. Genes and pathways involved
486 in anabolism, such as *GH*, *IGF1*, translation and oxidative phosphorylation, were differentially expressed.
487 Their inhibition is among the best-documented life-prolonging interventions in a wide range of short-
488 lived model organisms (Table 2). Surprisingly, however, we found that the expression of these
489 mechanisms was consistently higher in slower-aging breeders than in faster-aging non-breeders. This
490 indicates that even basic molecular mechanisms of the aging process known from short-lived species
491 cannot easily be transferred to long-lived species. In particular, this applies to the role of the GH/IGF1
492 axis, which has in recent years been unilaterally described as harmful [81, 82, 106]. In addition, special
493 features of the mole-rats could also contribute to the explanation of the unexpected result that genes
494 and processes differentially expressed between reproductive statuses were also strongly altered during
495 the evolution of the mole-rats [113]. Another intriguing possibility is that, in line with the hormesis
496 hypothesis [93], moderate harmful effects of anabolic processes can be hyper-compensated for by up-
497 regulation of pathways such as proteasomes, P53-signaling and antioxidant defense against ROS that we
498 observed in slower-aging breeders as well.

499 Furthermore, our work provides evidence that the HPA stress axis is a key regulator for the observed
500 downstream effects, including the lifespan difference. The effects are likely to be triggered by
501 differential expression of the gene *MC2R* coding for the ACTH receptor resulting in an altered stress
502 response in breeders vs. non-breeders. This is supported by the fact that cortisol levels in the non-
503 breeders are elevated. Furthermore, the set of direct and indirect target genes of the glucocorticoid
504 receptors is strongly affected by differential expression, and numerous known downstream effects of
505 glucocorticoid excess have been demonstrated for non-breeders, such as muscle weakness, weight gain,
506 and GH/IGF1 axis impairment. Overall, this evidence suggests that *MC2R* and other genes along the
507 described signalling pathway are promising targets for possible interventions in aging research.

Methods

Animal care and sampling

All animals were housed in glass terraria with dimensions adjusted to the size of the family (min. 40 cm × 60 cm) in the Department of General Zoology, Faculty of Biosciences, University of Duisburg-Essen. The terraria are filled with a 5 cm layer of horticultural peat or sawdust. Tissue paper strips, tubes, and solid shelters were provided as bedding/nesting materials and environmental enrichment. Potatoes and carrots are supplied ad libitum as stable food, supplemented with apples, lettuce, and cereals. *Fukomys* mole-rats do not drink free water. Temperature was kept fairly constant at 26± 1 °C, and humidity, at approximately 40 %. The daily rhythm was set to 12 hours darkness and 12 hours light.

New breeder pairs (new families) were established between March and May 2014. Each new family was founded by two unfamiliar, randomly chosen adult non-breeders of similar age (min/max/mean: 1.56/6.5/3.58 years in *F. mechowii*; 1.8/5.4/3.1 years in *F. micklemi*) and opposite sex and were taken from already existing separate colonies. These founder animals were moved to a new terrarium in which they were permanently mated. In both species, more than 80 % of these new pairs reproduced within the first 12 months (total number of offspring by the end of the year 2016, 82 *F. micklemi* and 81 *F. mechowii*). Only founders with offspring were subsequently assigned to the breeder cohort; founders without offspring were excluded from the study. Non-breeders remained in their natal family together with both parents and other siblings.

F. mechowii were sampled in five distinct sampling sessions between March 2015 and winter 2016/2017. F. *micklemi* were sampled in three distinct sampling sessions between November 2016 and July 2017. In both species, females were killed 4 to 6 months later than their male mates to ensure that

these breeder females were neither pregnant nor lactating at the time of sampling, in order to exclude additional uncontrolled variables.

Before sampling, animals were anaesthetized with 6 mg/kg ketamine combined with 2.5 mg/kg xylazine [114]. Once the animals lost their pedal withdrawal reflex, 1 to 2 ml of blood was collected by cardiac puncture, and the animals were killed by surgical decapitation. Blood samples (100 µl) were collected in RNAprotect Animal Blood reagent (Qiagen, Venlo, Netherlands). Tissue samples –hippocampus, hypothalamus, pituitary gland, thyroid, heart, skeletal muscle (M. quadriceps femoris), lateral skin, small intestine (ileum), upper colon, spleen, liver, kidney, adrenal gland, testis, and ovary – were transferred to RNAlater (Qiagen, Venlo, Netherlands) immediately after dissection and, following incubation, were stored at -80°C until analysis.

Animal housing and tissue collection were compliant with national and state legislation (breeding allowances 32-2-1180-71/328 and 32-2-11-80-71/345; ethics/animal experimentation approval 84–02.04.2013/A164, Landesamt für Natur-, Umwelt- und Verbraucherschutz Nordrhein-Westfalen).

RNA preparation and sequencing

For all tissues except blood, RNA was purified with the RNeasy Mini Kit (Qiagen) according to the manufacturer's protocol. Blood RNA was purified with the RNeasy Protect Animal Blood Kit (Qiagen). Kidney and heart samples were treated with proteinase K before extraction, as recommended by the manufacturer. Library preparation was performed using the TruSeq RNA v2 kit (Illumina, San Diego, USA) which includes selection of poly-adenylated RNA molecules. RNA-seq was performed by single-end sequencing with 51 cycles in high-output mode on a HiSeq 2500 sequencing system (Illumina) and with at least 20 million reads per sample, as described in Table S9. Read data for *F. mechowii* and *F. micklemi* were deposited as European Nucleotide Archive study with the ID PRJEB29798 (Table S9).

Read mapping and quantification

It was ensured for all samples that the results of the respective sequencing passed “per base” and “per sequence” quality checks of FASTQC [115]. The reads were then mapped against previously published and with human gene symbols annotated *F. mechowii* and *F. micklemi* transcriptome data [24, 113]. For both species, only the longest transcript isoform per gene was used; this is the method of choice for selecting a representative variant in large-scale experiments [116] (Data S2, S3). This selection resulted in 15,864 reference transcripts (genes) for *F. mechowii* and in 16,400 for *F. micklemi*. After mapping and quantification, we further analyzed only those reference transcripts whose gene symbols were present in the transcript catalogs of both species – this was the case for 15,199 transcripts (the size of the union was 17,065). As mapping algorithm “bwa aln” of the Burrows-Wheeler Aligner (BWA) [117] was used, allowing no gaps and a maximum of two mismatches in the alignment. Only those reads that could be uniquely mapped to the respective gene were used for quantification. Read counts per gene and sample can be found in Data S4. As another check, we ensured that all samples exhibited a Pearson correlation coefficient of at least 90% in a pairwise comparison based on $\log_2$-transformed read counts against all other samples of the same experimental group as defined by samples that were equal in the tissue as well as the species, sex, and reproductive status of the source animal.

Differentially expressed genes analysis

P-values for differential gene expression and fold-changes were determined with DESeq2 [118] and a multi-factorial design. The DESeq2-algorithm also includes strict filtering based on a normalized mean gene count that makes further pre-filtering unnecessary [118]. Therefore, those genes whose read count was zero for all examined samples were removed before further analysis, thereby reducing the number of analyzed genes to 15,181. The multi-factorial design means that, separately for each tissue, we input the read count data of samples across species, sex, and reproductive status into DESeq2 for each

sample. This allowed DESeq2 to perform DEG-analysis between the two possible states of each of the variables by controlling for additional variance in the other two variables. This approach resulted in a four-times higher sample size than with an approach that would have been based on comparisons of two experimental groups, each of which would be equal in tissue, species, sex, and reproductive status. It is known that the statistical power in RNA-seq experiments can increase considerably with sample size [119]. P-values were corrected for multiple testing with the Benjamini-Hochberg correction [120] (false discovery rate – FDR).

The results of the DEG-analysis can be found in Data S5-S7.

Enrichment analysis on pathway and cross-tissue level

Let $(p_1^t, \dots p_n^t)$ represent the p-values obtained from differential gene expression analysis in the tissue corresponding with index t and the indices $1, \dots, n$ corresponding to the examined genes. Forthermore, let $(p_{x_1}^t, \dots., p_{x_m}^t)$, with $1 \leq x_i \leq n$ and $1 \leq i \leq m$, represent the p-values of genes with the indices $X = (x_1, \dots, x_m)$ belonging to a corresponding pathway that is tested for enrichment of differential expression signals. To determine the enrichment p-values at the pathway-level, we calculated the test statistic $\mathcal{F}_X^t$ for the gene indices X in tissue index t according to Fisher's method for combining p-values also known as Brown's method:

$$\mathcal{F}_X^t = -2 * \sum_{i=1}^{m} \log_e(p_{x_i}^t)$$

Because p-values at the gene level were, as is common in RNA-seq experiments [121], not equally distributed, we empirically estimated the null distribution of the test statistic for each pathway instead of using the χ^2-distribution as frequently suggested in the literature [122-124]. This was done by calculating $\mathcal{F}_{X^j}^t$ for 1,000 random drawings, each without replacement, $X^j = (x_1^j, \dots, x_m^j)$, with

$1 \leq x_k^j \leq n,\ 1 \leq j \leq 1000$. If the resulting p-value was zero (meaning $\forall\ 1 \leq j \leq 1000$: $\mathcal{F}_X^t > F_{X^j}^t$), the procedure was repeated with 10,000 and 100,000 random drawings, respectively. In addition, the indices X were divided into X_{up} and X_{down}, depending on whether their fold-change was > 1 or < 1 in breeder vs. non-breeder comparison, and $\mathcal{F}_{X_{up}}^t$ and $\mathcal{F}_{X_{down}}^t$ calculated. The ratio $\frac{\mathcal{F}_{X_{up}}^t}{\mathcal{F}_{X_{down}}^t}$ was used as an indicator for functional up- or down-regulation of the corresponding pathway (Fig. 4, Fig. S3, S4). Using this approach, enrichment p-values were estimated for all KEGG-pathways [30] and MSigDB-hallmarks [31], as well as across all examined tissues (Data S8, S9). In addition, the procedure was applied to test whether the known 300 direct and 1300 indirect glucocorticoid receptor target genes [55] were enriched for status-dependent differential expression signals (Tables S7, S8).

Similarly, cross-tissue DEG-p-values were weighted with a modified test statistic (c.f. [125]). Given the definitions from above, we calculated the weighted cross-tissue test statistic $\mathcal{F}^g$ for the gene g as follows:

$$\mathcal{F}^g = |2 * \sum_{t=1}^{l} (\log_e(p_g^t) * w_g^t)|$$

$$\text{with } w_g^t = \frac{\overline{expr}_g^t * sgn(logFC_g^t)}{\sum_{t=1}^{l} \overline{expr}_g^t}$$

where $logFC_g^t$ and $\overline{expr}_g^t$ are the logarithmized fold-change between reproductive states and normalized mean expression (across sexes, species, and reproductive status) for the gene with index g and tissue with index t – both calculated by DESeq2 [118] –, sgn is the signum function, and l is the number of examined tissues. The reasoning for using this test statistic was as follows: For the weighted cross-tissue analysis, we assumed that the gene serves the same function throughout the entire organism. Therefore, the test statistic given above weights the p-values of the various tissues by the

613 respective expression levels in those tissues. This ensures that, weighting e. g., a ubiquitously expressed
614 genes such as *TP53* is relatively equally across tissues, whereas for typical steroid hormone-biosynthesis
615 genes, such as *CYP11A1*, the endocrine tissue results determine almost exclusively the weighted cross-
616 tissue p-value. Furthermore, the test statistic rewards, based on the mentioned assumption, consistency
617 in the direction of gene regulation throughout tissues. All calculated values for $logFC_g^t$, $\overline{expr}_g^t$, p_g^t, as
618 well as the resulting $\mathcal{F}^g$ and p-values, can be found in Data S10.

619 Finally, weighted cross-tissue enrichment p-values at the pathway level were estimated by applying the
620 above-described method at the pathway level (based on test statistic $\mathcal{F}$) to the gene level weighted
621 cross-tissue p-values.

622 P-values were corrected for multiple testing with the Benjamini-Hochberg correction [120] (FDR).

623 Weighted gene co-expression network analysis

624 We used the WGCNA R package to perform weighted correlation network analysis [33] of all 636
625 samples at once. We followed the authors' usage recommendation by choosing a soft power threshold
626 based on scale-free topology and mean connectivity development (we chose power=26 with a soft R^2 of
627 0.92 and a mean connectivity of 38.6), using biweight midcorrelation, setting maxPOutliers to 0.1, and
628 using "signed" both as network and topological overlap matrix type. The maximum block size was
629 chosen such that the analysis was performed with a single block and the minimum module size was set
630 to 30. The analysis divided the genes into 26 modules, of which 5 were enriched for reproductive status
631 DEGs based on Fisher's exact test and an FDR threshold of 0.05. Those 5 modules were tested for
632 enrichment among KEGG-pathways [30] with the same test and significance threshold (Table S10). In
633 addition, module eigengenes were determined and clustered (Table S10). Then the topological overlap
634 matrix that resulted from the WGCNA analysis ($TOM = [tom_{i,j}]$, where the row indices $1 \leq i \leq$

$|examined\ genes|$ correspond to genes and the column indices $1 \leq j \leq |examined\ samples|$ correspond to samples) was used to determine pairwise connectivity between all KEGG-pathways that showed differential expression at the weighted cross-tissue level (Fig. S5). Based on the definition of connectivity of genes in a WGCNA analysis [33], we defined the connectivity between two sets of indices X and Y each corresponding to genes as $k_{X,Y} = \sum_{x \in X \setminus Y} \sum_{y \in Y \setminus X} tom_{x,y}$. P-values for the connectivities were determined against null distributions that were empirically estimated by determining for each pair X and Y the connectivities of 10,000 pairs of each $|X|$ and $|Y|$ randomly drawn indices (without replacement), respectively. Since "signed" was used as the network and topological overlap matrix type, the tests were one-sided.

Other analysis steps

Hierarchical clustering (Fig. S2) was performed based on Pearson correlation coefficients of log_2-transformed read counts between all sample pairs using the complete-linkage method [126]. The principal variant component analysis (Fig. 2A) was performed with the pvca package from Bioconductor [127] and a minimum demanded percentile value of the amount of the variabilities, that the selected principal components needs to explain, of 0.5. Enrichments of DEGs among genes enlisted in the Digital Aging Atlas database ([29], Data S11) were determined with Fisher's exact test, the Benjamini-Hochberg method (FDR) [120] for multiple test correction, and a significance threshold of 0.05. Pathway visualization (Fig. S6-S9) was performed with Pathview [128]. For the direction analysis of *Fukomys* reproductive status DEGs in previous experiments in naked-mole rats and guinea pigs, we examined those 10 tissues that were examined in all species (Table S6, Data S12). Separately for each tissue and combination of species – naked mole-rat or guinea pig – and sex, we determined how many *Fukomys* reproductive status DEGs were up-regulated or down-regulated. We also performed two-sided binomial tests on each of these number pairs with a hypothesized success probability of 0.5. Furthermore, for

each combination of species and sex, two-sided exact binomial tests using 0.5 as parameter were performed based on the sums of up-regulated and down-regulated genes across tissues (Table S6). For enrichment analysis of direct and indirect glucocorticoid receptor target genes, mouse mRNA RefSeq IDs from Phuc Le et al. [55] were translated to human Entrez IDs and gene symbols via Ensembl Biomart (Data S13). To statistically analyze the weight gain of the animals during the experiment, we used a type II ANOVA with status, species, sex, and age as independent variables (Table S2); the weight gain, defined as the difference in weights at beginning and the end of the experiment, as dependent variable (Fig. 6B); and no interaction terms. If interaction terms were also used for the model, the p-value for the difference in means between breeders and non-breeders changed from $7.49*10^{-3}$, as reported above, to $7.46*10^{-6}$.

Bone density measurements

Frozen carcasses of all *F. micklemi* that had been part of the transcriptome study were scanned with a self-shielded desktop small- animal computer tomography scanner (X-CUBE, Molecubes, Belgium). The x-ray source was a tungsten anode (peak voltage, 50 kVp; tube current, 350 µA; 0.8 mm aluminum filter). The detector was a cesium iodide (CsI) flat-panel, building up a screen with 1536 x 864 pixels. Measurements were carried for individual 120 ms exposures, with angular sampling intervals of 940 exposures per rotation, for to a total of 7 rotations and a total exposure time of 789.6 seconds.

First, we first performed a calibration of the reconstructed CT data in terms of equivalent mineral density. For this purpose, we used a bone density calibration phantom (BDC; QRM GmbH, Moehrendorf, Germany) composed of five cylindrical inserts with a diameter of 5 mm containing various densities of calcium hydroxyapatite (CaHA) surrounded by epoxy resin on a cylindrical shape. The nominal values of CaHA were 0, 100, 200, 400, and 800 mg HA/cm^3, corresponding to a density of 1.13, 1.16, 1.25, 1.64,and 1.90 g/cm^3 (certified with an accuracy of ± 0.5 %). The BDC was imaged and reconstructed with

the same specifications as each probe. From the reconstructed Hounsfield Units, a linear relationship was determined against the known mineral concentrations.

Reconstruction of the acquired computer tomography data was carried with an Image Space Reconstruction Algorithm, and spatial resolution was limited to the 100 µm voxel matrix reconstruction. Spherical regions of interest (radius, 0.7 mm) were drawn on the sagittal plane of vertebrae T12, L1, and L2. Care was taken to include all cancellous bone, excluding the cortical edges. Average Hounsfield Unit values were computed on the calibration curve to finally retrieve equivalent densities of the regions of interest.

Statistical analysis was performed using general linear models with bone density (Hounsfield Units) as dependent variable, age (in days) as continuous covariate, and reproductive status and sex as nominal cofactors. Models were calculated for each vertebra individually (individual models) and across all three vertebrae (full model); in this latter case, vertebral number was added as additional categorial cofactor. In all models, only main effects were calculated, no interactions. Analyses were performed with IBM SPSS version 25 (Fig. 6C, Table S11).

Abbreviations

ANOVA – analysis of variance

ACTH – adrenocorticotropic hormone

DAA – Digital Aging Atlas

DEG – differentially expressed gene

DHEA – Dehydroepiandrosterone

FDR – false discovery rate

KEGG – Kyoto Encyclopedia of Genes and Genomes

MSigDB – Molecular Signatures Database

Declarations

Ethics approval and consent to participate

Animal housing and tissue collection were compliant with national and state legislation (breeding allowances 32-2-1180-71/328 and 32-2-11-80-71/345, ethics/animal experimentation approval 84–02.04.2013/A164, Landesamt für Natur-, Umwelt- und Verbraucherschutz Nordrhein-Westfalen).

Consent for publication

Not applicable.

Availability of data and materials

Read datasets generated during the current study are available in the European Nucleotide Archive, study ID: PRJEB29798.

Competing interests

The authors declare that they have no competing interests.

Funding

This work was funded by the Deutsche Forschungsgemeinschaft (DFG, PL 173/8-1 and DA 992/3-1). The funders had no role in study design, data collection and analysis, decision to publish, or preparation of the manuscript.

Authors' contributions

PD, MP, and KS conceived the project (with input from SB) and acquired the funding. PD, KS, and AS monitored the implementation of the project. PD, SB, HB, and PVD were responsible for housing the animals and implementing concrete mating schemes. PD, SB, ST, MGo, MS, JK, and PFC performed physiological measurements. PD, YH, KS, AS, SB, and MB sampled the animals. MG supervised library preparation and sequencing. AS, KS, and MB analyzed the data. AS, PD, MP, KS, SH, and PK interpreted the data and drafted the manuscript concept. All authors wrote and approved the manuscript.

Acknowledgments

We thank Ivonne Görlich, Christiane Vole, and Klaus Huse for excellent assistance in the preparation of biological samples. We thank Konstantin Riege for fruitful discussions on the analysis of the data. We thank Debra Weih and Flo Witte for proofreading the manuscript.

Figure legends

Figure 1. Motivation (A) and principle of the experimental setup (B).

A) For both species of the *Fukomys* genus that were examined in this study – *F. mechowii* and *F. micklem*i – it was shown that, in captivity, breeder live significantly longer than non-breeders. Lifespan data were redrawn from Dammann & Burda and Dammann et al. [13, 14]. **B)** Schematic overview of animal treatments. Non-breeders (open shapes) are offspring of the breeder pair of their family (filled shapes) and do not mate with other members of the same family because of incest avoidance in *Fukomys* [12]. Therefore, non-breeders of opposite sexes were taken from different families – labeled as "Family A" (blue) and "Family B" (red) – and permanently housed in a separate terrarium. The two unrelated animals mated with each other, thus producing offspring and becoming breeders of the new

741 "Family C" (green). In addition to the animals that were promoted to be slower-aging breeders, age-
742 matched controls that remained in the faster-aging non-breeders of "Family A" and "Family B" were
743 included in our study – in most cases full siblings (ideally litter mates) of the respective new breeders.
744 After at least two years and two pregnancies in "Family C", breeders from "Family C" and their controls
745 from Colonies A and B were put to death, and tissues were sampled for later analysis, that included
746 identification of differentially expressed genes (DEGs). The shown experimental scheme was conducted
747 with 5 to 7 (median 6) specimens per cohort (defined by breeding status, sex, species) and 12 to 15
748 tissues (median 14) per specimen: in total, 46 animals and 636 samples.

749 **Figure 2.** Total variance distribution (A) and numbers of differentially expressed genes (B).

750 **A)** Relative contribution of the model factors (breeding status, sex, species, tissue) and their
751 combinations (:) to the total variance in the examined data set. The relative contributions were
752 determined by principal variance component analysis. **B)** Numbers of identified differentially expressed
753 genes per tissue and model factor (first column, species; second, sex; third, status). Stacked bars
754 indicate the proportions of up- and down-regulated genes (red and green, respectively; directions: *F.*
755 *mechowii* vs. *F. micklemi*, female vs. male, breeder vs. non-breeder).

756 **Figure 3.** Assessment of the aging relevance of genes that are differentially expressed between breeders
757 and non-breeders.

758 **A)** For each tissue, we separately tested whether the identified differentially expressed genes between
759 status groups significantly overlapped with the genes within the Digital Aging Atlas database (Fisher's
760 exact test, FDR < 0.05). Significant overlaps were found for three tissues: adrenal gland, ovary and
761 pituitary gland. The Venn-diagram depicts the overlaps of these three tissues with the Digital Aging Atlas
762 and with each other (** : FDR < 0.01; *** : FDR < 0.001). **B)** A similar experiment comparing the

763 transcriptomes of breeders versus non-breeders was recently conducted in naked mole-rats (NMRs) and
764 guinea pig (GPs) [7]. For NMR there is also evidence that breeders have a (slightly) longer lifespan than
765 non-breeders, whereas for GP the opposite is assumed [7, 27]. Across ten tissues that were examined in
766 both studies, the analysis determined whether status-dependent differentially expressed genes
767 identified in the current study were regulated in the same or opposite direction in NMR and GP (Table
768 S6). The listed p-values (two-sided binomial exact test; hypothesized probability, 0.5) describe how
769 extremely the ratio of genes expressed in the same and opposite directions deviates from a 50:50 ratio.
770 Green and orange indicate the majority and minority of genes within a comparison, respectively. Figure
771 created with BioRender.com.

772 **Figure 4.** Pathways and metabolic functions enriched for status-dependent differential gene expression.
773 Shown are all Kyoto Encyclopedia of Genes and Genomes (KEGG) pathways (**A**) and Molecular Signatures
774 Database (MSigDB) hallmarks (**B**) that are enriched for differential gene expression between breeders
775 and non-breeders at the weighted cross-tissue level (false discovery rate [FDR], < 0.1). The numbers
776 within the cells give the FDR, i.e., the multiple testing corrected p-value, for the respective
777 pathway/hallmark and tissue. As indicated by the color key, red and green stand for up- or down-
778 regulated in breeders, respectively. White indicates a pathway/hallmark that is significantly affected by
779 differential expression and whose signals for up- and down-regulation are approximately balanced. Dark
780 colors up to black mean that there is little or no evidence that the corresponding pathway/hallmark is
781 affected by differential gene expression. Figures S3 and S4 provide detailed overviews of all
782 pathways/hallmarks that are enriched in at least one tissue for status-dependent differential expression
783 signals.

784 **Figure 5.** Model of the stress axis as a key mechanism for status-dependent lifespan differences in
785 *Fukomys*. From a wide range of mammals, including humans [52], dogs [129], horses [130], cats [131],

786 and guinea pigs [132], it is known that chronic glucocorticoid excess leads to a number of pathologic
787 symptoms that largely overlap with those of aging and result in considerably higher mortality rates for
788 affected individuals [53#808]. The most common cause of chronic glucocorticoid excess is excessive
789 secretion of the adrenocorticotropic hormone (ACTH) by the pituitary gland. ACTH is transported via the
790 blood to the adrenal cortex where it binds to the ACTH-receptor (ACTHR; encoded by the gene *MC2R*)
791 which induces the production of glucocorticoids, especially cortisol. Glucocorticoids are transported to
792 the various tissues, where they exert their effect by activating the glucocorticoid receptor (NR3C1) that
793 acts as a transcription factor and regulates hundreds of genes. The constant overuse of this
794 transcriptional pattern eventually leads to the listed symptoms. Our hypothesis is that the permanent,
795 high expression of the ACTH-receptor in *Fukomys* non-breeders causes effects similar to those known
796 from overproduction of the hormone. In line with this hypothesis, i) cortisol levels are increased in non-
797 breeders and ii) target genes of the glucocorticoid-receptor are highly enriched for status-dependent
798 differential gene expression. Furthermore, the animals were examined for common symptoms of
799 chronic glucocorticoid excess: iii) non-breeders gained more weight during the experiment than
800 breeders, iv) exhibited lower bone density at the end of the experiment, and v) lower gene expression
801 in the GH-/IGF1 axis than breeders.

802 **Figure 6.** *MC2R* gene expression and physiological measurements. **A)** Gene expression of *MC2R*, coding
803 for the ACTH receptor, in breeders and non-breeders of *Fukomys mechowii* and *Fukomys micklemi*. **B)**
804 Weight gain of the animals during the experiment. **C)** Measured optical densities of vertebra T12 of
805 *Fukomys micklemi* breeders and non-breeders. Red, breeders; blue, non-breeders; filled, *F. mechowii*;
806 unfilled, *F. micklemi*; circles, females; squares, males; dashed line, median. Statistically significant
807 differences between breeders and non-breeders were determined with A) DESeq2 [118] and B+C)
808 analysis of variance with status, species, sex, and age as independent variables (see methods).

Additional files

Supplement Figures

Figure S1. Overview of the tissues examined in this study with a schematic mole-rat representation.

Figure S2. Clustering of the 636 examined samples. Clustering was performed based on the Euclidian distance of logarithmized pairwise Pearson read count correlations using the UPGMA method.

Figure S3. Full overview of Kyoto Encyclopedia of Genes and Genomes (KEGG) pathways that are enriched for status-dependent differential gene expression.

Figure S4. Full overview of Molecular Signatures Database (MsigDB) hallmarks that are enriched for status-dependent differential gene expression.

Figure S5. Pairwise connectivity of metabolic pathways that are enriched for status-dependent differential gene expression at the cross-tissue level.

Figure S6. Status-dependent regulation of Kyoto Encyclopedia of Genes and Genomes (KEGG) pathway hsa00140 Steroid hormone biosynthesis at the cross-tissue level.

Figure S7. Status-dependent regulation of Kyoto Encyclopedia of Genes and Genomes (KEGG) pathway hsa05016 Huntington's disease at the cross-tissue level.

Figure S8. Status-dependent regulation of Kyoto Encyclopedia of Genes and Genomes (KEGG) pathway hsa05012 Parkinson's disease at the cross-tissue level.

Figure S9. Status-dependent regulation of Kyoto Encyclopedia of Genes and Genomes (KEGG) pathway hsa050160 Alzheimer's disease at the cross-tissue level.

Supplement Tables

Table S1. Overview of number of samples that were examined with regard to status, sex, species, and tissue.

Table S2. Animal description.

Table S3. Overview of the tissues that were successfully sampled for each type of animal.

Table S4. Pairing scheme: *F. mechowii*.

Table S5. Pairing scheme: *F. micklemi*.

Table S6. Analysis of the direction of status-dependent differentially expressed genes that were identified in this study (two *Fukomys* species) in similar experiments with naked mole-rats and guinea pigs (Bens et al. 2018, https://www.ncbi.nlm.nih.gov/pmc/articles/PMC6090939/).

Table S7. Analysis of status-dependent differential gene expression enrichment on glucocorticoid receptor target genes that were determined by Phuc Le at al. 2005 (https://www.ncbi.nlm.nih.gov/pmc/articles/PMC1186734/), using chromatin immunoprecipitation (CHIP).

Table S8. Analysis of status-dependent differential gene expression enrichment on glucocorticoid receptor target genes that were determined by Phuc Le at al. 2005 (https://www.ncbi.nlm.nih.gov/pmc/articles/PMC1186734/), using a differential gene expression analysis.

Table S9. Sample description.

Table S10. WGCNA module clustering and functional enrichment analysis regarding these modules.

Table S11. Bone density measurements.

Supplement Data

Data S1. (zip) For each KEGG pathway and MSigDB hallmark that was detected to be significantly (FDR < 0.1) enriched for status-dependent differential expression at the weighted cross-tissue level, the data set contains a *.tsv file with the genes that form the respective pathway/hallmark sorted by their individual contribution to the enrichment. The files also provide an overview of the p-values and fold-changes of those genes in those tissues in which the genes are expressed most highly.

Data S2. (fa.gz) Transcript isoforms of *F. mechowii* used for read mapping.

Data S3. (fa.gz) Transcript isoforms of *F. micklemi* used for read mapping.

Data S4. (tsv.gz) Raw read counts for all 17,065 genes and 636 samples that were analyzed in this study using RNA-seq.

Data S5. (zip) DESeq2 results for status-dependent gene expression (direction: breeder/non-breeder). The data set contains one *.tsv file per analyzed tissue.

Data S6. (zip) DESeq2 results for sex-dependent gene expression (direction: female/male). The data set contains one *.tsv file per analyzed tissue.

Data S7. (zip) DESeq2 results for species-dependent gene expression (direction: mechowii/micklemi). The data set contains one *.tsv file per analyzed tissue.

Data S8. (zip) Enrichment analysis results for status-dependent gene expression on KEGG pathways. The data set contains one *.tsv file per analyzed tissue, as well as an additional *.tsv file for the weighted cross-tissue level results.

Data S9. (zip) Enrichment analysis results for status-dependent gene expression on MSigDB hallmarks. The data set contains one *.tsv file per analyzed tissue, as well as an additional *.tsv file for the weighted cross-tissue level results.

Data S10. (tsv.gz) Overview of the weighted cross-tissue differential gene expression analysis. Contains all p-values, fold-changes, and mean expression values for all genes across all tissues as well as the weighted, combined cross-tissue test statistics, p-values, and fold-changes for all genes.

Data S11. (tsv) Genes of the Digital Aging Atlas used in this study.

Data S12. (zip) Comparison of status-dependent differentially expressed genes with results of an earlier, similar study involving naked mole-rats (NMRs) and guinea pigs (GPs). The data set contains one *.tsv file for each of the ten tissues that were examined in both studies. Each *.tsv file lists the differentially expressed genes for the respective tissue as identified in this study with the determined FDRs and fold-changes, as well as the fold-changes determined in the earlier study using naked mole-rats and guinea pigs.

Data S13. (zip) Glucocorticoid receptor target genes that were determined by Phuc Le *et al.* and tested in this study for enrichment of status-dependent differential gene expression. The data set contains one *.tsv file each for target genes determined via chromatin immunoprecipitation (CHIP) and differential gene expression analysis. Phuc Le et al. determined differentially expressed genes between mice that were treated with exogenous glucocorticoids and untreated controls. The relevant table columns from Phuc Le et al. were added by human gene symbol and Entrez IDs that were used for enrichment analysis.

References

1. Keller L, Jemielity S: **Social insects as a model to study the molecular basis of ageing.** *Exp Gerontol* 2006, **41:**553-556.

2. Parker JD, Parker KM, Sohal BH, Sohal RS, Keller L: **Decreased expression of Cu-Zn superoxide dismutase 1 in ants with extreme lifespan.** *Proc Natl Acad Sci U S A* 2004, **101:**3486-3489.
3. Austad SN: **Comparative biology of aging.** *J Gerontol A Biol Sci Med Sci* 2009, **64:**199-201.
4. Dammann P: **Slow aging in mammals-Lessons from African mole-rats and bats.** *Semin Cell Dev Biol* 2017, **70:**154-163.
5. Salmon AB, Leonard S, Masamsetti V, Pierce A, Podlutsky AJ, Podlutskaya N, Richardson A, Austad SN, Chaudhuri AR: **The long lifespan of two bat species is correlated with resistance to protein oxidation and enhanced protein homeostasis.** *FASEB J* 2009, **23:**2317-2326.
6. Austad SN: **Candidate bird species for use in aging research.** *ILAR J* 2011, **52:**89-96.
7. Bens M, Szafranski K, Holtze S, Sahm A, Groth M, Kestler HA, Hildebrandt TB, Platzer M: **Naked mole-rat transcriptome signatures of socially suppressed sexual maturation and links of reproduction to aging.** *BMC Biol* 2018, **16:**77.
8. Sichilima AM, Faulkes CG, Bennett NC: **Field evidence for aseasonality of reproduction and colony size in the Afrotropical giant mole-rat Fukomys mechowii (Rodentia: Bathyergidae).** *African Zoology* 2008, **43:**144-149.
9. Skliba J, Mazoch V, Patzenhauerova H, Hrouzková E, Lövy M, Kott O, Šumbera R: **A maze-lover's dream: Burrow architecture, natural history and habitat characteristics of Ansell's mole-rat (Fukomys anselli).** *MAMMALIAN BIOLOGY* 2012, **77:**420-427.
10. Jarvis JU, Bennett NC: **Eusociality has evolved independently in two genera of bathyergid mole-rats — but occurs in no other subterranean mammal.** *Behavioral Ecology and Sociobiology* 1993, **33:**253-260.
11. Scharff A, Locker-Gruetjen O, Kawalika M, Burda H: **Natural history of the Giant mole-rat, Cryptomys mechowi (Rodentia: Bathyergidae) from Zambia.** *Journal of Mammalogy* 2001, **82:**1002-1015.
12. Burda H: **Individual recognition and incest avoidance in eusocial common mole-rats rather than reproductive suppression by parents.** *Experientia* 1995, **51:**411-413.
13. Dammann P, Burda H: **Sexual activity and reproduction delay ageing in a mammal.** *Curr Biol* 2006, **16:**R117-118.
14. Dammann P, Sumbera R, Massmann C, Scherag A, Burda H: **Extended longevity of reproductives appears to be common in Fukomys mole-rats (Rodentia, Bathyergidae).** *PLoS One* 2011, **6:**e18757.
15. Carmona JJ, Michan S: **Biology of Healthy Aging and Longevity.** *Rev Invest Clin* 2016, **68:**7-16.
16. Valenzano DR, Terzibasi E, Genade T, Cattaneo A, Domenici L, Cellerino A: **Resveratrol Prolongs Lifespan and Retards the Onset of Age-Related Markers in a Short-Lived Vertebrate.** *Current Biology* 2006, **16:**296-300.
17. Johnson SC, Rabinovitch PS, Kaeberlein M: **mTOR is a key modulator of ageing and age-related disease.** *Nature* 2013, **493:**338-345.
18. Morimoto RI, Cuervo AM: **Protein homeostasis and aging: taking care of proteins from the cradle to the grave.** *J Gerontol A Biol Sci Med Sci* 2009, **64:**167-170.
19. Harman D: **Aging: a theory based on free radical and radiation chemistry.** *J Gerontol* 1956, **11:**298-300.
20. Harman D: **Aging: overview.** *Ann N Y Acad Sci* 2001, **928:**1-21.
21. Dammann P, Sell DR, Begall S, Strauch C, Monnier VM: **Advanced glycation end-products as markers of aging and longevity in the long-lived Ansell's mole-rat (Fukomys anselli).** *J Gerontol A Biol Sci Med Sci* 2012, **67:**573-583.

22. Schmidt CM, Blount JD, Bennett NC: **Reproduction is associated with a tissue-dependent reduction of oxidative stress in eusocial female Damaraland mole-rats (Fukomys damarensis).** *PLoS One* 2014, **9:**e103286.
23. Henning Y, Vole C, Begall S, Bens M, Broecker-Preuss M, Sahm A, Szafranski K, Burda H, Dammann P: **Unusual ratio between free thyroxine and free triiodothyronine in a long-lived mole-rat species with bimodal ageing.** *PLoS One* 2014, **9:**e113698.
24. Sahm A, Bens M, Henning Y, Vole C, Groth M, Schwab M, Hoffmann S, Platzer M, Szafranski K, Dammann P: **Higher gene expression stability during aging in long-lived giant mole-rats than in short-lived rats.** *Aging (Albany NY)* 2018, **10:**3938-3956.
25. Sherman PW, Jarvis JUM: **Extraordinary life spans of naked mole-rats (Heterocephalus glaber).** *Journal of Zoology* 2002, **258:**307-311.
26. Buffenstein R: **Negligible senescence in the longest living rodent, the naked mole-rat: insights from a successfully aging species.** *J Comp Physiol B* 2008, **178:**439-445.
27. Ruby JG, Smith M, Buffenstein R: **Naked Mole-Rat mortality rates defy gompertzian laws by not increasing with age.** *Elife* 2018, **7**.
28. Dammann P, Scherag A, Zak N, Szafranski K, Holtze S, Begall S, Burda H, Kestler HA, Hildebrandt T, Platzer M: **Comment on 'Naked mole-rat mortality rates defy Gompertzian laws by not increasing with age'.** *Elife* 2019, **8**.
29. Craig T, Smelick C, Tacutu R, Wuttke D, Wood SH, Stanley H, Janssens G, Savitskaya E, Moskalev A, Arking R, de Magalhaes JP: **The Digital Ageing Atlas: integrating the diversity of age-related changes into a unified resource.** *Nucleic Acids Res* 2015, **43:**D873-878.
30. Kanehisa M, Furumichi M, Tanabe M, Sato Y, Morishima K: **KEGG: new perspectives on genomes, pathways, diseases and drugs.** *Nucleic Acids Res* 2017, **45:**D353-D361.
31. Liberzon A, Birger C, Thorvaldsdottir H, Ghandi M, Mesirov JP, Tamayo P: **The Molecular Signatures Database (MSigDB) hallmark gene set collection.** *Cell Syst* 2015, **1:**417-425.
32. Hofmann JW, Zhao X, De Cecco M, Peterson AL, Pagliaroli L, Manivannan J, Hubbard GB, Ikeno Y, Zhang Y, Feng B, et al: **Reduced expression of MYC increases longevity and enhances healthspan.** *Cell* 2015, **160:**477-488.
33. Langfelder P, Horvath S: **WGCNA: an R package for weighted correlation network analysis.** *BMC Bioinformatics* 2008, **9:**559.
34. Schiaffino S, Mammucari C: **Regulation of skeletal muscle growth by the IGF1-Akt/PKB pathway: insights from genetic models.** *Skelet Muscle* 2011, **1:**4.
35. Jung HJ, Suh Y: **Regulation of IGF -1 signaling by microRNAs.** *Front Genet* 2014, **5:**472.
36. Junnila RK, List EO, Berryman DE, Murrey JW, Kopchick JJ: **The GH/IGF-1 axis in ageing and longevity.** *Nat Rev Endocrinol* 2013, **9:**366-376.
37. Cannata D, Vijayakumar A, Fierz Y, LeRoith D: **The GH/IGF-1 axis in growth and development: new insights derived from animal models.** *Adv Pediatr* 2010, **57:**331-351.
38. Lozier NR, Kopchick JJ, de Lacalle S: **Relative Contributions of Myostatin and the GH/IGF-1 Axis in Body Composition and Muscle Strength.** *Front Physiol* 2018, **9:**1418.
39. Raisingani M, Preneet B, Kohn B, Yakar S: **Skeletal growth and bone mineral acquisition in type 1 diabetic children; abnormalities of the GH/IGF-1 axis.** *Growth Horm IGF Res* 2017, **34:**13-21.
40. Bodart G, Goffinet L, Morrhaye G, Farhat K, de Saint-Hubert M, Debacq-Chainiaux F, Swine C, Geenen V, Martens HJ: **Somatotrope GHRH/GH/IGF-1 axis at the crossroads between immunosenescence and frailty.** *Ann N Y Acad Sci* 2015, **1351:**61-67.
41. Carotti S, Guarino MPL, Valentini F, Porzio S, Vespasiani-Gentilucci U, Perrone G, Zingariello M, Gallo P, Cicala M, Picardi A, Morini S: **Impairment of GH/IGF-1 Axis in the Liver of Patients with HCV-Related Chronic Hepatitis.** *Horm Metab Res* 2018, **50:**145-151.

42. Liu D, Ahmet A, Ward L, Krishnamoorthy P, Mandelcorn ED, Leigh R, Brown JP, Cohen A, Kim H: **A practical guide to the monitoring and management of the complications of systemic corticosteroid therapy.** *Allergy Asthma Clin Immunol* 2013, **9:**30.
43. Miller WL, Auchus RJ: **The molecular biology, biochemistry, and physiology of human steroidogenesis and its disorders.** *Endocr Rev* 2011, **32:**81-151.
44. Wang J, Mitsche MA, Lutjohann D, Cohen JC, Xie XS, Hobbs HH: **Relative roles of ABCG5/ABCG8 in liver and intestine.** *J Lipid Res* 2015, **56:**319-330.
45. Liu Y, Ordovas JM, Gao G, Province M, Straka RJ, Tsai MY, Lai CQ, Zhang K, Borecki I, Hixson JE, et al: **The SCARB1 gene is associated with lipid response to dietary and pharmacological interventions.** *J Hum Genet* 2008, **53:**709-717.
46. Hammer F, Subtil S, Lux P, Maser-Gluth C, Stewart PM, Allolio B, Arlt W: **No Evidence for Hepatic Conversion of Dehydroepiandrosterone (DHEA) Sulfate to DHEA: In Vivo and in Vitro Studies.** *The Journal of Clinical Endocrinology & Metabolism* 2005, **90:**3600-3605.
47. Rutkowski K, Sowa P, Rutkowska-Talipska J, Kuryliszyn-Moskal A, Rutkowski R: **Dehydroepiandrosterone (DHEA): hypes and hopes.** *Drugs* 2014, **74:**1195-1207.
48. Celec P, Starka L: **Dehydroepiandrosterone - is the fountain of youth drying out?** *Physiol Res* 2003, **52:**397-407.
49. Baulieu EE: **Dehydroepiandrosterone (DHEA): a fountain of youth?** *J Clin Endocrinol Metab* 1996, **81:**3147-3151.
50. Walker JJ, Spiga F, Gupta R, Zhao Z, Lightman SL, Terry JR: **Rapid intra-adrenal feedback regulation of glucocorticoid synthesis.** *J R Soc Interface* 2015, **12:**20140875.
51. Chabre O: **[Cushing syndrome: Physiopathology, etiology and principles of therapy].** *Presse Med* 2014, **43:**376-392.
52. Ferrau F, Korbonits M: **Metabolic comorbidities in Cushing's syndrome.** *Eur J Endocrinol* 2015, **173:**M133-157.
53. Etxabe J, Vazquez JA: **Morbidity and mortality in Cushing's disease: an epidemiological approach.** *Clin Endocrinol (Oxf)* 1994, **40:**479-484.
54. Gjerstad JK, Lightman SL, Spiga F: **Role of glucocorticoid negative feedback in the regulation of HPA axis pulsatility.** *Stress* 2018, **21:**403-416.
55. Phuc Le P, Friedman JR, Schug J, Brestelli JE, Parker JB, Bochkis IM, Kaestner KH: **Glucocorticoid receptor-dependent gene regulatory networks.** *PLoS Genet* 2005, **1:**e16.
56. Tatar M, Bartke A, Antebi A: **The endocrine regulation of aging by insulin-like signals.** *Science* 2003, **299:**1346-1351.
57. Chahal HS, Drake WM: **The endocrine system and ageing.** *J Pathol* 2007, **211:**173-180.
58. Jones CM, Boelaert K: **The Endocrinology of Ageing: A Mini-Review.** *Gerontology* 2015, **61:**291-300.
59. Allolio B, Arlt W: **DHEA treatment: myth or reality?** *Trends in Endocrinology & Metabolism* 2002, **13:**288-294.
60. Webb SJ, Geoghegan TE, Prough RA, Michael Miller KK: **The biological actions of dehydroepiandrosterone involves multiple receptors.** *Drug Metab Rev* 2006, **38:**89-116.
61. Maggio M, Lauretani F, Ceda GP, Bandinelli S, Ling SM, Metter EJ, Artoni A, Carassale L, Cazzato A, Ceresini G, et al: **Relationship between low levels of anabolic hormones and 6-year mortality in older men: the aging in the Chianti Area (InCHIANTI) study.** *Arch Intern Med* 2007, **167:**2249-2254.
62. Traish AM, Kang HP, Saad F, Guay AT: **Dehydroepiandrosterone (DHEA)--a precursor steroid or an active hormone in human physiology.** *J Sex Med* 2011, **8:**2960-2982; quiz 2983.

63. Samaras N, Samaras D, Forster A, Frangos E, Philippe J: **[Age related dehydroepiandrosterone decrease: clinical significance and therapeutic interest].** *Rev Med Suisse* 2015, **11:**321-324.
64. Burkhardt T, Schmidt NO, Vettorazzi E, Aberle J, Mengel M, Flitsch J: **DHEA(S)--a novel marker in Cushing's disease.** *Acta Neurochir (Wien)* 2013, **155:**479-484; discussion 484.
65. Fridmanis D, Roga A, Klovins J: **ACTH Receptor (MC2R) Specificity: What Do We Know About Underlying Molecular Mechanisms?** *Front Endocrinol (Lausanne)* 2017, **8:**13.
66. Becker DE: **Basic and clinical pharmacology of glucocorticosteroids.** *Anesth Prog* 2013, **60:**25-31; quiz 32.
67. Newfield RS: **ACTH receptor blockade: a novel approach to treat congenital adrenal hyperplasia, or Cushing's disease.** *Med Hypotheses* 2010, **74:**705-706.
68. Imai T, Sarkar D, Shibata A, Funahashi H, Morita-Matsuyama T, Kikumori T, Ohmori S, Seo H: **Expression of adrenocorticotropin receptor gene in adrenocortical adenomas from patients with Cushing syndrome: possible contribution for the autonomous production of cortisol.** *Ann Surg* 2001, **234:**85-91.
69. Lin L, Hindmarsh PC, Metherell LA, Alzyoud M, Al-Ali M, Brain CE, Clark AJ, Dattani MT, Achermann JC: **Severe loss-of-function mutations in the adrenocorticotropin receptor (ACTHR, MC2R) can be found in patients diagnosed with salt-losing adrenal hypoplasia.** *Clin Endocrinol (Oxf)* 2007, **66:**205-210.
70. Beuschlein F, Fassnacht M, Klink A, Allolio B, Reincke M: **ACTH-receptor expression, regulation and role in adrenocortial tumor formation.** *Eur J Endocrinol* 2001, **144:**199-206.
71. Ochi A, Adachi T, Inokuchi K, Ogawa K, Nakamura Y, Chiba Y, Kawasaki S, Onishi Y, Onuma Y, Munetsugu Y, et al: **Effects of Aging on the Coagulation Fibrinolytic System in Outpatients of the Cardiovascular Department.** *Circ J* 2016, **80:**2133-2140.
72. Benayoun BA, Pollina EA, Singh PP, Mahmoudi S, Harel I, Casey KM, Dulken BW, Kundaje A, Brunet A: **Remodeling of epigenome and transcriptome landscapes with aging in mice reveals widespread induction of inflammatory responses.** *Genome Res* 2019, **29:**697-709.
73. Lowe G, Rumley A: **The relevance of coagulation in cardiovascular disease: what do the biomarkers tell us?** *Thromb Haemost* 2014, **112:**860-867.
74. Annibaldi A, Meier P: **Checkpoints in TNF-Induced Cell Death: Implications in Inflammation and Cancer.** *Trends Mol Med* 2018, **24:**49-65.
75. Pistritto G, Trisciuoglio D, Ceci C, Garufi A, D'Orazi G: **Apoptosis as anticancer mechanism: function and dysfunction of its modulators and targeted therapeutic strategies.** *Aging (Albany NY)* 2016, **8:**603-619.
76. Baig S, Seevasant I, Mohamad J, Mukheem A, Huri HZ, Kamarul T: **Potential of apoptotic pathway-targeted cancer therapeutic research: Where do we stand?** *Cell Death Dis* 2016, **7:**e2058.
77. Hands SL, Proud CG, Wyttenbach A: **mTOR's role in ageing: protein synthesis or autophagy?** *Aging (Albany NY)* 2009, **1:**586-597.
78. Bartke A: **Growth Hormone and Aging: Updated Review.** *World J Mens Health* 2019, **37:**19-30.
79. Rudman D, Feller AG, Nagraj HS, Gergans GA, Lalitha PY, Goldberg AF, Schlenker RA, Cohn L, Rudman IW, Mattson DE: **Effects of human growth hormone in men over 60 years old.** *N Engl J Med* 1990, **323:**1-6.
80. Longo VD, Antebi A, Bartke A, Barzilai N, Brown-Borg HM, Caruso C, Curiel TJ, de Cabo R, Franceschi C, Gems D, et al: **Interventions to Slow Aging in Humans: Are We Ready?** *Aging Cell* 2015, **14:**497-510.
81. Pitt JN, Kaeberlein M: **Why is aging conserved and what can we do about it?** *PLoS Biol* 2015, **13:**e1002131.

82. Lopez-Otin C, Blasco MA, Partridge L, Serrano M, Kroemer G: **The hallmarks of aging.** *Cell* 2013, **153:**1194-1217.
83. Kurosu H, Yamamoto M, Clark JD, Pastor JV, Nandi A, Gurnani P, McGuinness OP, Chikuda H, Yamaguchi M, Kawaguchi H, et al: **Suppression of aging in mice by the hormone Klotho.** *Science* 2005, **309:**1829-1833.
84. Baumgart M, Priebe S, Groth M, Hartmann N, Menzel U, Pandolfini L, Koch P, Felder M, Ristow M, Englert C, et al: **Longitudinal RNA-Seq Analysis of Vertebrate Aging Identifies Mitochondrial Complex I as a Small-Molecule-Sensitive Modifier of Lifespan.** *Cell Syst* 2016, **2:**122-132.
85. Hipkiss AR: **On why decreasing protein synthesis can increase lifespan.** *Mech Ageing Dev* 2007, **128:**412-414.
86. Saez I, Vilchez D: **The Mechanistic Links Between Proteasome Activity, Aging and Age-related Diseases.** *Curr Genomics* 2014, **15:**38-51.
87. Perez VI, Buffenstein R, Masamsetti V, Leonard S, Salmon AB, Mele J, Andziak B, Yang T, Edrey Y, Friguet B, et al: **Protein stability and resistance to oxidative stress are determinants of longevity in the longest-living rodent, the naked mole-rat.** *Proc Natl Acad Sci U S A* 2009, **106:**3059-3064.
88. Rodriguez KA, Edrey YH, Osmulski P, Gaczynska M, Buffenstein R: **Altered Composition of Liver Proteasome Assemblies Contributes to Enhanced Proteasome Activity in the Exceptionally Long-Lived Naked Mole-Rat.** *PLOS ONE* 2012, **7:**e35890.
89. Pride H, Yu Z, Sunchu B, Mochnick J, Coles A, Zhang Y, Buffenstein R, Hornsby PJ, Austad SN, Perez VI: **Long-lived species have improved proteostasis compared to phylogenetically-related shorter-lived species.** *Biochem Biophys Res Commun* 2015, **457:**669-675.
90. Starkov AA: **The role of mitochondria in reactive oxygen species metabolism and signaling.** *Ann N Y Acad Sci* 2008, **1147:**37-52.
91. Balaban RS, Nemoto S, Finkel T: **Mitochondria, oxidants, and aging.** *Cell* 2005, **120:**483-495.
92. Bieging KT, Mello SS, Attardi LD: **Unravelling mechanisms of p53-mediated tumour suppression.** *Nat Rev Cancer* 2014, **14:**359-370.
93. Ristow M: **Unraveling the truth about antioxidants: mitohormesis explains ROS-induced health benefits.** *Nat Med* 2014, **20:**709-711.
94. Schielke CKM, Burda H, Henning Y, Okrouhlik J, Begall S: **Higher resting metabolic rate in long-lived breeding Ansell's mole-rats (Fukomys anselli).** *Front Zool* 2017, **14:**45.
95. van Heemst D: **Insulin, IGF-1 and longevity.** *Aging Dis* 2010, **1:**147-157.
96. Elibol B, Kilic U: **High Levels of SIRT1 Expression as a Protective Mechanism Against Disease-Related Conditions.** *Front Endocrinol (Lausanne)* 2018, **9:**614.
97. Kwon Y, Kim J, Lee CY, Kim H: **Expression of SIRT1 and SIRT3 varies according to age in mice.** *Anat Cell Biol* 2015, **48:**54-61.
98. Satoh A, Brace CS, Rensing N, Cliften P, Wozniak DF, Herzog ED, Yamada KA, Imai S: **Sirt1 extends life span and delays aging in mice through the regulation of Nk2 homeobox 1 in the DMH and LH.** *Cell Metab* 2013, **18:**416-430.
99. Burnett C, Valentini S, Cabreiro F, Goss M, Somogyvari M, Piper MD, Hoddinott M, Sutphin GL, Leko V, McElwee JJ, et al: **Absence of effects of Sir2 overexpression on lifespan in C. elegans and Drosophila.** *Nature* 2011, **477:**482-485.
100. Edrey YH, Salmon AB: **Revisiting an age-old question regarding oxidative stress.** *Free Radic Biol Med* 2014, **71:**368-378.
101. Feng Z, Lin M, Wu R: **The Regulation of Aging and Longevity: A New and Complex Role of p53.** *Genes Cancer* 2011, **2:**443-452.

102. Giannakou ME, Goss M, Junger MA, Hafen E, Leevers SJ, Partridge L: **Long-lived Drosophila with overexpressed dFOXO in adult fat body.** *Science* 2004, **305:**361.
103. Carmona-Gutierrez D, Hughes AL, Madeo F, Ruckenstuhl C: **The crucial impact of lysosomes in aging and longevity.** *Ageing Res Rev* 2016, **32:**2-12.
104. Dillin A, Hsu AL, Arantes-Oliveira N, Lehrer-Graiwer J, Hsin H, Fraser AG, Kamath RS, Ahringer J, Kenyon C: **Rates of behavior and aging specified by mitochondrial function during development.** *Science* 2002, **298:**2398-2401.
105. Copeland JM, Cho J, Lo T, Jr., Hur JH, Bahadorani S, Arabyan T, Rabie J, Soh J, Walker DW: **Extension of Drosophila life span by RNAi of the mitochondrial respiratory chain.** *Curr Biol* 2009, **19:**1591-1598.
106. Bartke A: **Somatic growth, aging, and longevity.** *NPJ Aging Mech Dis* 2017, **3:**14.
107. Tacutu R, Craig T, Budovsky A, Wuttke D, Lehmann G, Taranukha D, Costa J, Fraifeld VE, de Magalhaes JP: **Human Ageing Genomic Resources: integrated databases and tools for the biology and genetics of ageing.** *Nucleic Acids Res* 2013, **41:**D1027-1033.
108. Delaney MA, Nagy L, Kinsel MJ, Treuting PM: **Spontaneous histologic lesions of the adult naked mole rat (Heterocephalus glaber): a retrospective survey of lesions in a zoo population.** *Vet Pathol* 2013, **50:**607-621.
109. Gorbunova V, Hine C, Tian X, Ablaeva J, Gudkov AV, Nevo E, Seluanov A: **Cancer resistance in the blind mole rat is mediated by concerted necrotic cell death mechanism.** *Proc Natl Acad Sci U S A* 2012, **109:**19392-19396.
110. Seluanov A, Gladyshev VN, Vijg J, Gorbunova V: **Mechanisms of cancer resistance in long-lived mammals.** *Nat Rev Cancer* 2018, **18:**433-441.
111. Berryman DE, Christiansen JS, Johannsson G, Thorner MO, Kopchick JJ: **Role of the GH/IGF-1 axis in lifespan and healthspan: lessons from animal models.** *Growth Horm IGF Res* 2008, **18:**455-471.
112. Milman S, Huffman DM, Barzilai N: **The Somatotropic Axis in Human Aging: Framework for the Current State of Knowledge and Future Research.** *Cell Metab* 2016, **23:**980-989.
113. Sahm A, Bens M, Szafranski K, Holtze S, Groth M, Gorlach M, Calkhoven C, Muller C, Schwab M, Kraus J, et al: **Long-lived rodents reveal signatures of positive selection in genes associated with lifespan.** *PLoS Genet* 2018, **14:**e1007272.
114. Garcia Montero A, Burda H, Begall S: **Chemical restraint of African mole-rats (Fukomys sp.) with a combination of ketamine and xylazine.** *Vet Anaesth Analg* 2015, **42:**187-191.
115. Andrews S: **FastQC A Quality Control tool for High Throughput Sequence Data.** *http://wwwbioinformaticsbabrahamacuk/projects/fastqc/*.
116. Ezkurdia I, Rodriguez JM, Carrillo-de Santa Pau E, Vazquez J, Valencia A, Tress ML: **Most highly expressed protein-coding genes have a single dominant isoform.** *J Proteome Res* 2015, **14:**1880-1887.
117. Li H, Durbin R: **Fast and accurate short read alignment with Burrows-Wheeler transform.** *Bioinformatics* 2009, **25:**1754-1760.
118. Love MI, Huber W, Anders S: **Moderated estimation of fold change and dispersion for RNA-seq data with DESeq2.** *Genome Biol* 2014, **15:**550.
119. Ching T, Huang S, Garmire LX: **Power analysis and sample size estimation for RNA-Seq differential expression.** *RNA* 2014, **20:**1684-1696.
120. Benjamini Y, Y. H: **Controlling the false discovery rate: A practical and powerful approach to multiple testing.** *Journal of the Royal Statistical Society Series B (Methodological)* 1995, **57:**289-300.

121. Väremo L, Nielsen J, Nookaew I: **Enriching the gene set analysis of genome-wide data by incorporating directionality of gene expression and combining statistical hypotheses and methods.** *Nucleic Acids Research* 2013, **41:**4378-4391.
122. Fridley BL, Jenkins GD, Biernacka JM: **Self-contained gene-set analysis of expression data: an evaluation of existing and novel methods.** *PloS one* 2010, **5:**e12693.
123. Evangelou M, Rendon A, Ouwehand WH, Wernisch L, Dudbridge F: **Comparison of Methods for Competitive Tests of Pathway Analysis.** *PLOS ONE* 2012, **7:**e41018.
124. Poole W, Gibbs DL, Shmulevich I, Bernard B, Knijnenburg TA: **Combining dependent P-values with an empirical adaptation of Brown's method.** *Bioinformatics (Oxford, England)* 2016, **32:**i430-i436.
125. Heard NA, Rubin-Delanchy P: **Choosing between methods of combining p-values.** *Biometrika* 2018, **105:**239-246.
126. Defays D: **An efficient algorithm for a complete link method.** *The Computer Journal* 1977, **20:**364-366.
127. Bushel P: **pvca: Principal Variance Component Analysis (PVCA).** 2013.
128. Luo W, Brouwer C: **Pathview: an R/Bioconductor package for pathway-based data integration and visualization.** *Bioinformatics* 2013, **29:**1830-1831.
129. Kooistra HS, Galac S: **Recent Advances in the Diagnosis of Cushing's Syndrome in Dogs.** *Topics in Companion Animal Medicine* 2012, **27:**21-24.
130. McCue PM: **Equine Cushing's disease.** *Vet Clin North Am Equine Pract* 2002, **18:**533-543, viii.
131. Meijer JC, Lubberink AA, Gruys E: **Cushing's syndrome due to adrenocortical adenoma in a cat.** *Tijdschr Diergeneeskd* 1978, **103:**1048-1051.
132. Zeugswetter F, Fenske M, Hassan J, Kunzel F: **Cushing's syndrome in a guinea pig.** *Vet Rec* 2007, **160:**878-880.

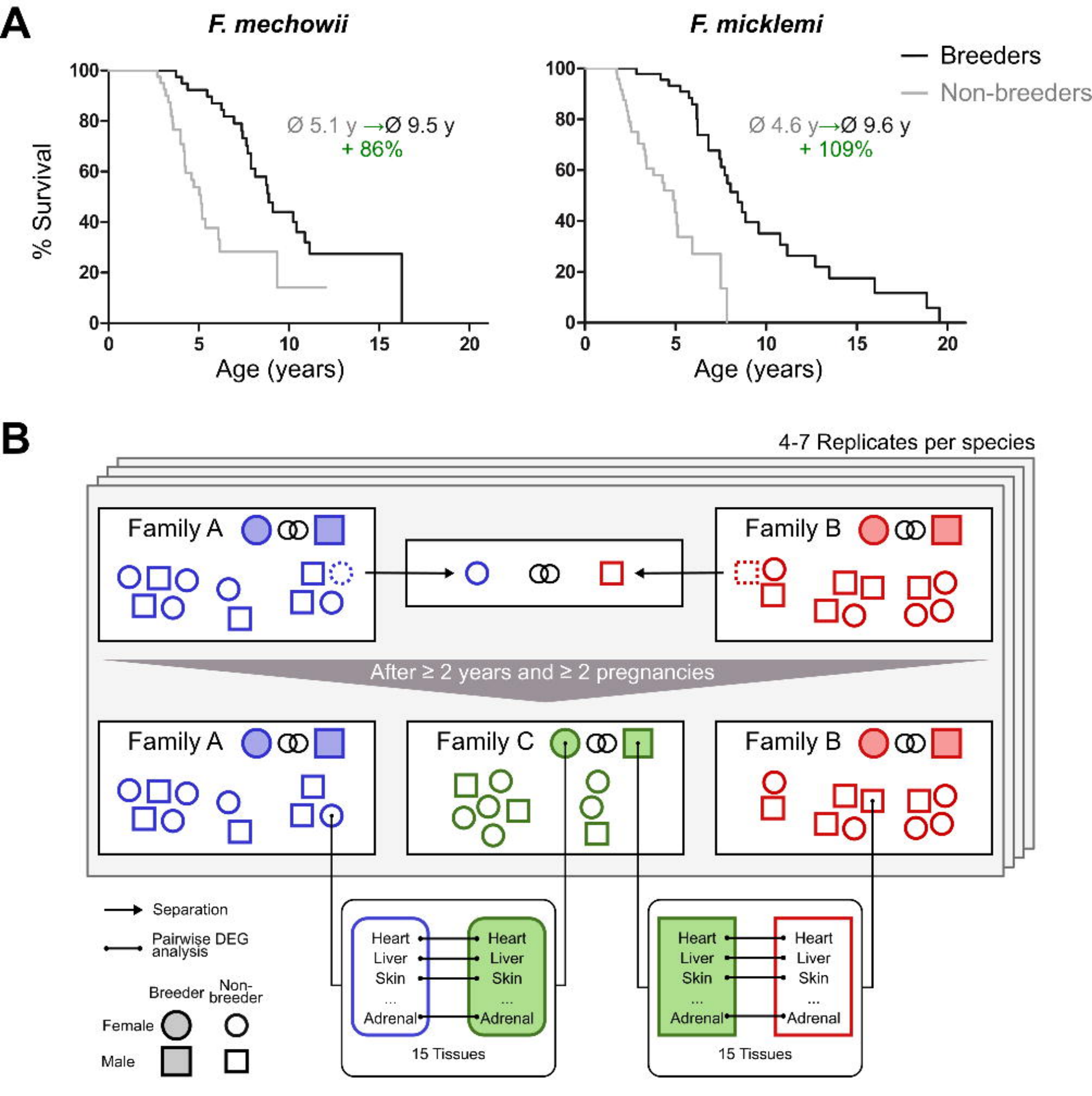
A
F. mechowii
F. micklemi
Breeders
Non-breeders
% Survival
Ø 5.1 y →Ø 9.5 y
+ 86%
Ø 4.6 y→Ø 9.6 y
+ 109%
Age (years)
Age (years)
B
4-7 Replicates per species
Family A
Family B
After ≥ 2 years and ≥ 2 pregnancies
Family A
Family C
Family B
Separation
Pairwise DEG analysis
Breeder
Non-breeder
Female
Male
Heart
Liver
Skin
...
Adrenal
15 Tissues
Heart
Liver
Skin
...
Adrenal
15 Tissues

A

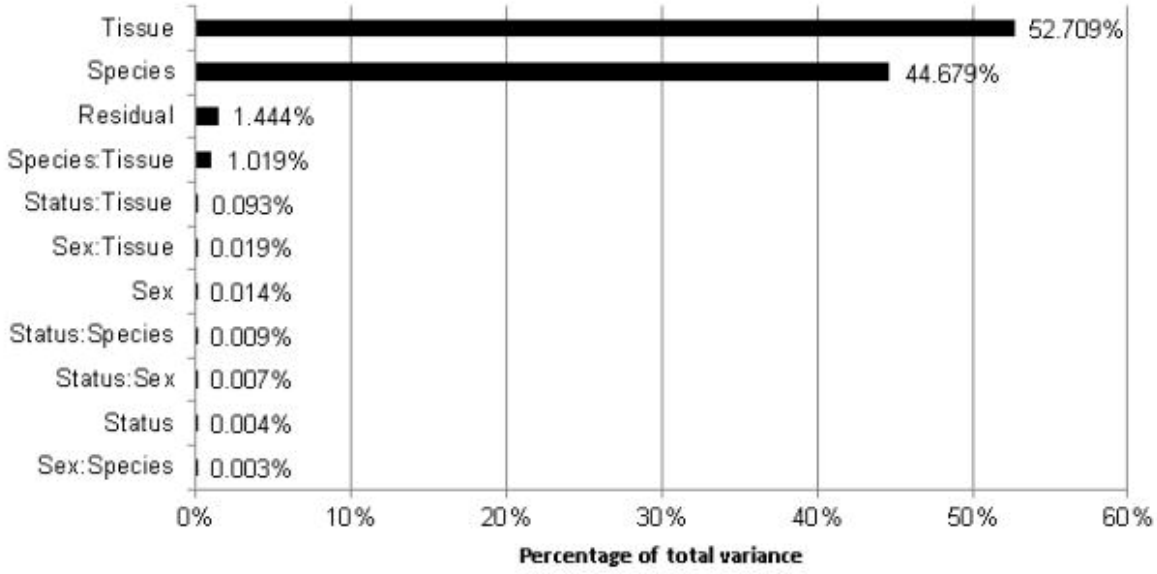
Tissue
Species
Residual
Species:Tissue
Status:Tissue
Sex:Tissue
Sex
Status:Species
Status:Sex
Status
Sex:Species
52.709%
44.679%
1.444%
1.019%
0.093%
0.019%
0.014%
0.009%
0.007%
0.004%
0.003%
0%
10%
20%
30%
40%
50%
60%
Percentage of total variance

B

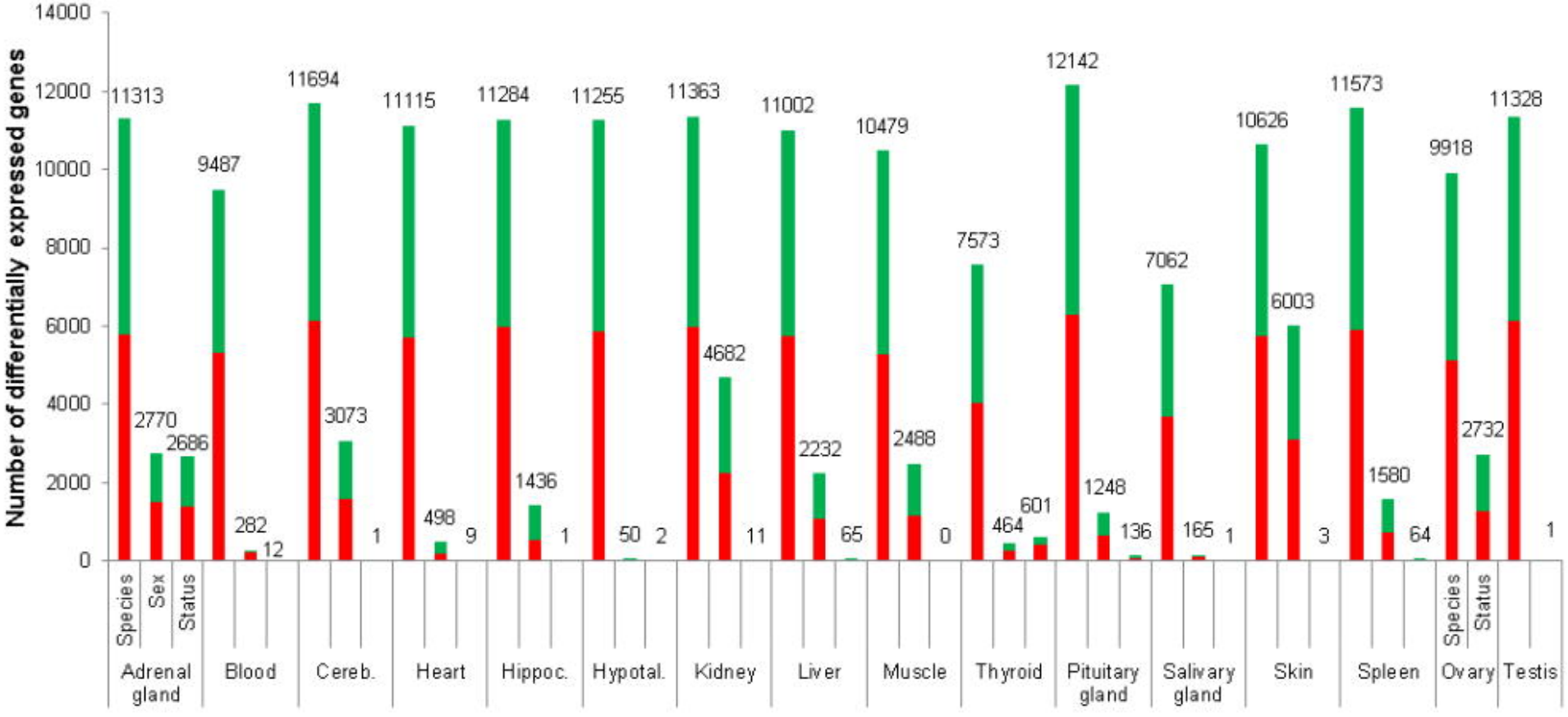
Number of differentially expressed genes
14000
12000
10000
8000
6000
4000
2000
0
11313
2770
2686
9487
282
12
11694
3073
1
11115
498
9
11284
1436
1
11255
50
2
11363
4682
11
11002
2232
65
10479
2488
0
7573
464
601
12142
1248
136
7062
165
1
10626
6003
3
11573
1580
64
9918
2732
11328
1
Species
Sex
Status
Adrenal gland
Blood
Cereb.
Heart
Hippoc.
Hypotal.
Kidney
Liver
Muscle
Thyroid
Pituitary gland
Salivary gland
Skin
Spleen
Species
Status
Ovary
Testis

A

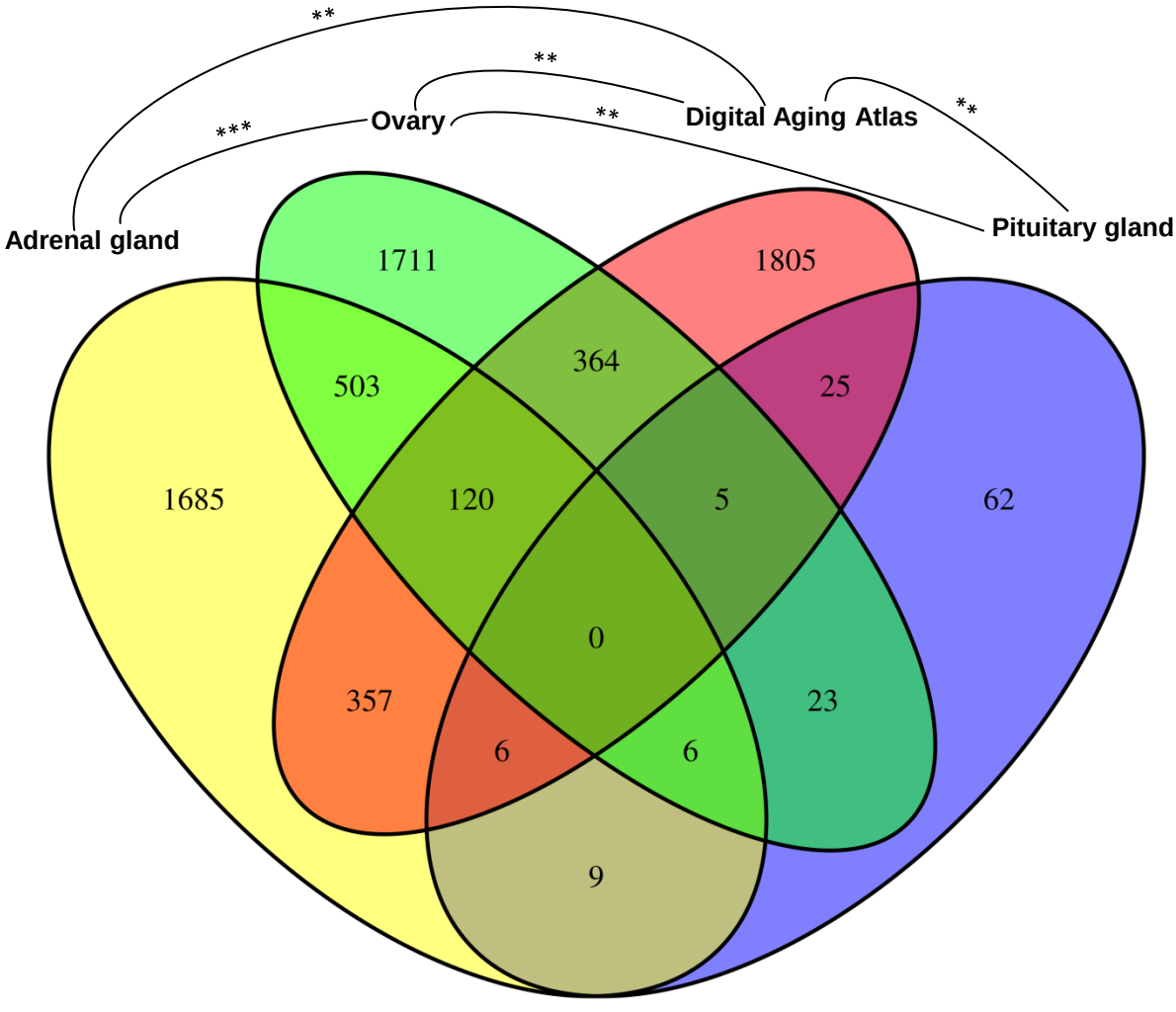

B

	NMR ♀	NMR ♂	GP ♀	GP ♂
Same	3561	2060	2521	1352
Opposite	2332	1225	3305	1917
P-value	$5.2*10^{-58}$	$1*10^{-44}$	$9*10^{-25}$	$4.7*10^{-23}$

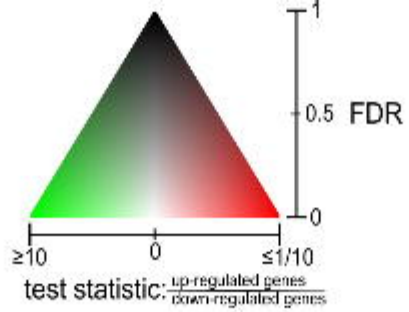

A

	Cross−tissue	Adrenal gland	Blood	Cerebellum	Heart	Hippocampus	Hypothalamus	Kidney	Liver	Muscle	Ovary	Pituitary gland	Salivary gland	Skin	Spleen	Testis	Thyroid
hsa03010 Ribosome	0.000	0.000	0.545	0.902	0.000	0.000	1.000	0.000	0.177	0.053	0.000	0.207	1.000	1.000	0.001	0.000	0.034
hsa05016 Huntington's disease	0.004	0.000	0.213	0.895	0.869	1.000	1.000	0.479	0.664	0.813	0.007	0.996	1.000	0.987	0.101	0.000	0.171
hsa03050 Proteasome	0.004	0.000	0.593	0.857	1.000	1.000	0.815	0.993	0.981	0.155	0.003	0.996	1.000	0.063	0.264	0.000	1.000
hsa00140 Steroid hormone biosynthesis	0.006	1.000	0.053	0.850	0.869	1.000	0.554	0.266	0.764	0.009	0.542	0.983	0.228	0.216	0.008	1.000	1.000
hsa05012 Parkinson's disease	0.018	0.000	0.053	0.883	1.000	0.684	1.000	0.098	0.991	0.868	0.002	0.996	1.000	0.929	0.118	0.002	0.263
hsa03008 Ribosome biogenesis in eukaryotes	0.023	0.094	0.655	0.814	0.725	1.000	0.652	0.975	0.380	0.524	0.722	0.996	0.982	0.987	0.118	0.713	0.388
hsa04260 Cardiac muscle contraction	0.031	0.408	0.602	0.850	0.598	1.000	0.968	0.820	0.931	0.367	0.605	0.163	0.982	0.932	0.149	0.537	0.538
hsa05010 Alzheimer's disease	0.031	0.000	0.087	0.857	0.889	1.000	0.919	0.076	0.897	0.650	0.019	0.996	0.982	0.889	0.239	0.009	0.263
hsa00190 Oxidative phosphorylation	0.033	0.000	0.593	0.914	0.954	1.000	1.000	0.813	0.991	0.402	0.002	0.996	1.000	0.682	0.239	0.011	0.263
hsa04976 Bile secretion	0.038	1.000	0.053	0.857	0.598	1.000	0.228	0.046	0.556	0.568	0.404	0.254	1.000	0.933	0.001	1.000	1.000
hsa00982 Drug metabolism − cytochrome P450	0.038	1.000	0.046	0.857	0.869	1.000	0.736	0.998	0.057	0.301	0.966	0.996	0.982	0.553	0.000	0.824	1.000
hsa04975 Fat digestion and absorption	0.038	1.000	0.213	0.643	0.925	1.000	0.324	0.975	0.897	0.189	0.179	0.358	0.982	0.520	0.062	1.000	1.000
hsa03013 RNA transport	0.053	0.023	0.644	0.814	0.598	1.000	1.000	0.820	0.897	0.418	0.719	0.996	1.000	0.936	0.239	0.537	0.309
hsa02010 ABC transporters	0.081	1.000	0.644	0.046	0.725	1.000	0.794	0.205	0.687	0.406	0.687	0.923	1.000	0.429	0.662	0.924	0.370

B

HALLMARK_MYC_TARGETS_V1	0.000	0.005	0.027	0.998	0.011	0.863	0.989	0.165	0.030	0.870	0.030	0.843	0.936	0.476	0.007	0.060	0.617
HALLMARK_XENOBIOTIC_METABOLISM	0.000	1.000	0.000	0.998	0.225	0.863	0.362	0.165	0.050	0.025	0.050	0.468	0.409	0.039	0.000	1.000	0.998
HALLMARK_OXIDATIVE_PHOSPHORYLATION	0.008	0.000	0.025	0.998	0.233	0.379	0.989	0.213	0.331	0.153	0.000	1.000	0.901	0.980	0.007	0.003	0.617
HALLMARK_HYPOXIA	0.012	0.896	0.014	0.998	0.225	0.423	0.989	0.956	0.135	0.784	0.050	0.057	0.550	0.000	0.153	1.000	0.780
HALLMARK_COAGULATION	0.020	1.000	0.000	0.998	0.450	0.921	0.937	0.274	0.094	0.308	0.888	0.820	0.969	0.864	0.000	1.000	0.998
HALLMARK_BILE_ACID_METABOLISM	0.025	1.000	0.025	0.998	0.418	0.370	0.989	0.539	0.322	0.039	0.497	1.000	0.243	0.980	0.007	0.835	0.617
HALLMARK_MYOGENESIS	0.028	1.000	0.060	0.998	0.005	0.150	0.017	0.602	0.323	0.005	0.842	0.000	0.150	0.998	0.980	0.987	0.780
HALLMARK_TNFA_SIGNALING_VIA_NFKB	0.028	1.000	0.002	0.998	0.546	0.423	0.989	0.970	0.165	0.286	1.000	0.146	0.550	0.000	0.007	1.000	0.885
HALLMARK_ANGIOGENESIS	0.028	0.039	0.161	0.998	0.625	0.578	0.669	0.165	0.331	0.933	0.858	0.853	0.741	0.252	0.050	0.945	0.998
HALLMARK_REACTIVE_OXIGEN_SPECIES_PATHWAY	0.092	0.017	0.799	0.998	0.307	0.578	0.989	0.748	0.820	0.029	0.114	0.145	0.178	0.705	0.808	0.600	0.998
HALLMARK_P53_PATHWAY	0.092	0.075	0.002	0.600	0.611	0.863	0.989	0.956	0.042	0.096	0.267	0.146	0.217	0.005	0.090	0.691	0.904
HALLMARK_APOPTOSIS	0.092	0.127	0.258	0.998	0.641	0.587	0.669	0.956	0.313	0.887	0.950	0.050	0.784	0.001	0.153	0.712	0.617
HALLMARK_PEROXISOME	0.096	0.771	0.253	0.650	0.191	0.225	0.862	0.539	0.050	0.153	0.842	1.000	0.894	0.980	0.007	0.382	0.060

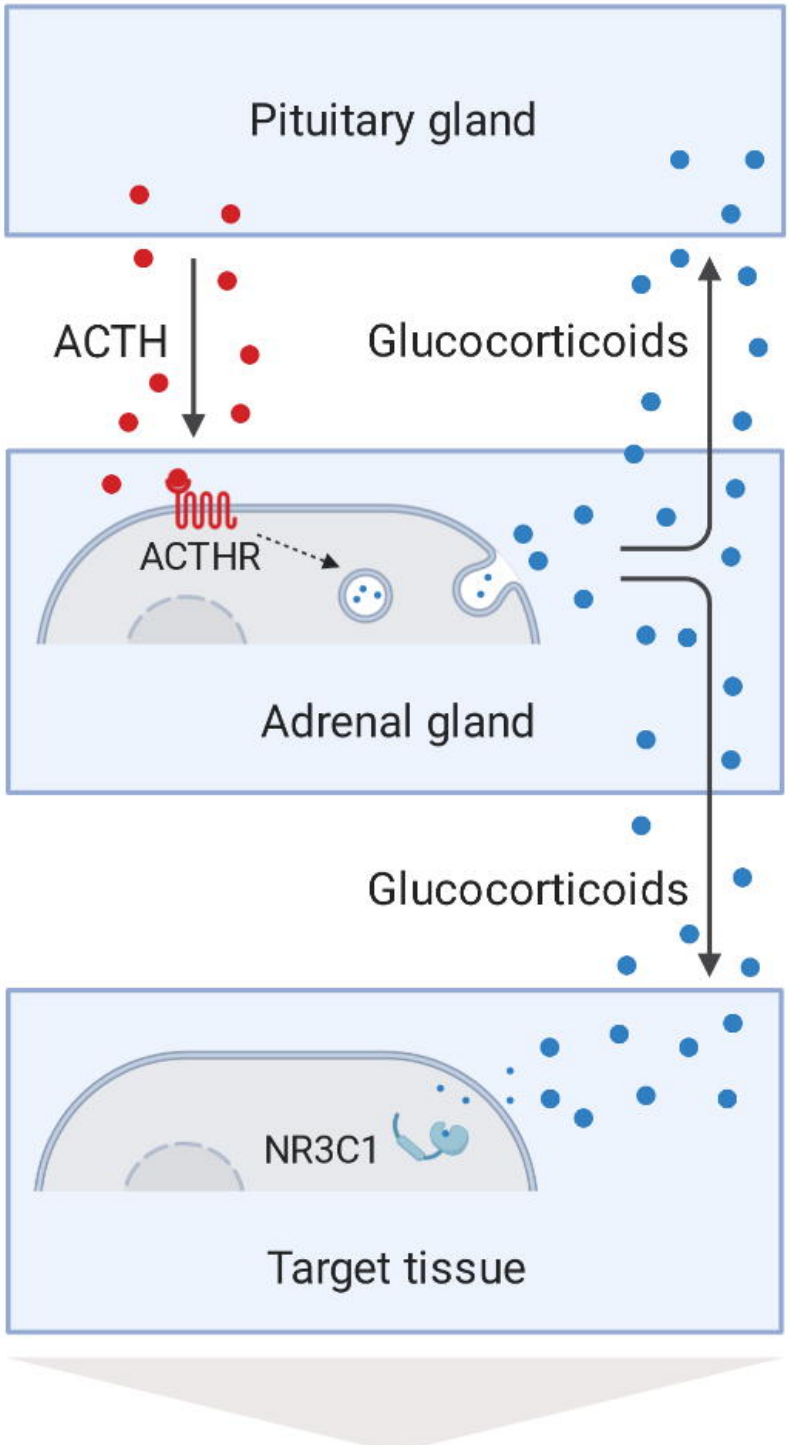

ACTHR (encoded by *MC2R*) is **up-regulated** in non-breeders

Cortisol level is **higher** in non-breeders

NR3C1 target genes are **differentially regulated** in non-breeders

Symptomes of glucocorticoid excess

- **Weight gain**
- **Loss of bone density**
- **GH-/IGF1 axis impairment**
- Muscle weakness
- Decreased fertility
- Immune suppression
- Cardiovascular disease

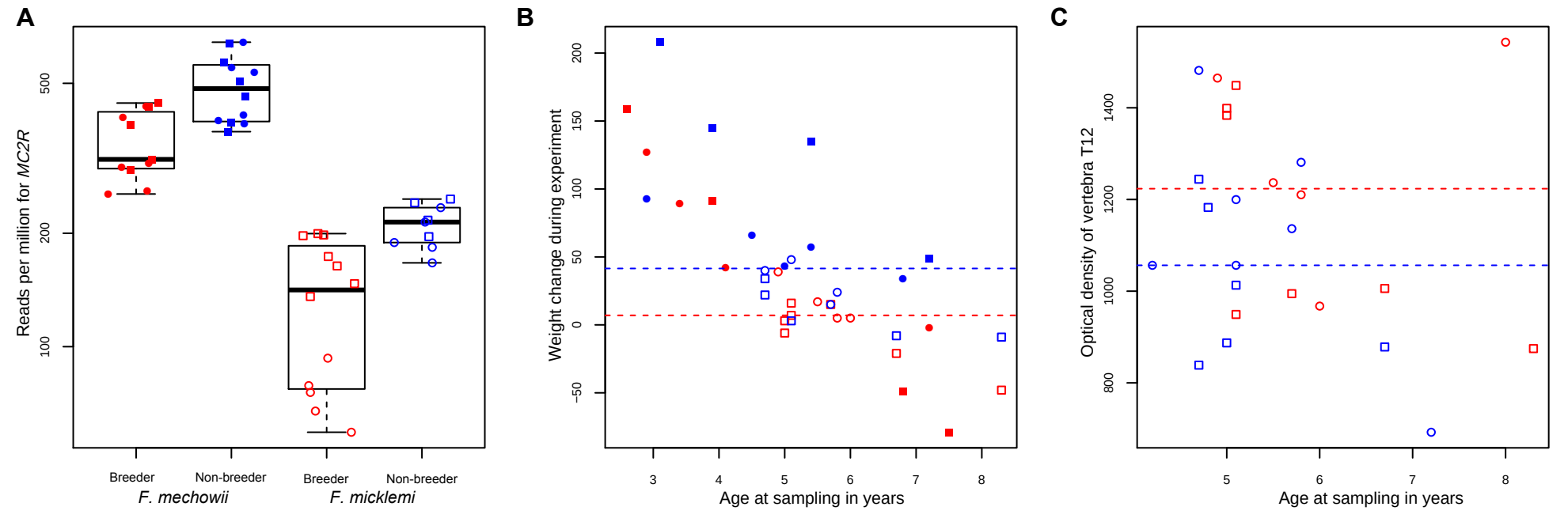
A
Reads per million for MC2R
100
200
500
Breeder
Non-breeder
Breeder
Non-breeder
F. mechowii
F. micklemi
B
Weight change during experiment
−50
0
50
100
150
200
3
4
5
6
7
8
Age at sampling in years
C
Optical density of vertebra T12
800
1000
1200
1400
5
6
7
8
Age at sampling in years